Industries, Inc. (Kamakura, Kanagawa, Japan). Lipopolysaccharide and Zymosan A from *Saccharomyces cerevisiae* were purchased from Sigma (St. Louis, MO).

Immunization and Infection

Five mice from each experimental group were anesthetized with diethyl ether and primarily immunized by dropping 1 μg of vaccine per mouse with various adjuvants into both nostril. Four weeks later, they were re-immunized in the same manner with the same adjuvant. For A/PR8 virus infection, two different infection protocols were used. Under the first protocol, each mouse was anesthetized and infected by intranasal application of 20 μl of virus suspension (1,000 PFU in PBS; 40 LD_{50}). This procedure induced total respiratory tract infection, which resulted in virus shedding from the nose and lungs, and led to death from viral pneumonia about 7 days later. Under the second protocol, anesthetized mice were infected by dropping 2 μl of virus suspension (1,000 PFU in PBS) into each nostril. The nasal-restricted volume (4 μl) of virus suspension induced nasally localized infection, which was not lethal. The nasal and lung wash virus titers were used as indices of protection in the upper and lower respiratory tracts of immunized mice, respectively. For infection with influenza A H5N1 virus, each mouse was anesthetized and 4 μl of PBS containing virus suspension with 1,000 PFU of H5N1 was administered intranasally (2 μl/nostril). The virus suspension remained in the local nasal area and could not enter the lung tissue, and the initial viral infection was limited to the nasal area, leading to death about 8 days later. H5N1 infection experiments were carried out in Biosafety Level 3 containment facilities, approved by the Guides for Animal Experiments Performed at National Institute of Infectious Diseases.

Measurement of Virus Titer and Antibody Titer

Serum, nasal washings, and bronchoalveolar washings were collected for measurement of virus titer and antibody titer from mice euthanized under anesthesia with chloroform. To collect nasal washings, a hypodermic needle was inserted into the posterior opening of the nasopharynx and 1 ml of PBS containing 0.1% bovine serum albumin was injected three times (1 ml total). Bronchoalveolar washings were collected by washing the trachea and lungs twice by injection of 1 ml PBS containing 0.1% BSA (2 ml total). The levels of IgA and IgG antibodies versus HA molecules purified from the A/PR8 viruses or NIBRG14 vaccine were determined by ELISA as described previously [Ichinohe et al., 2005, 2007a]. Briefly, ELISA was performed sequentially from the solid phase (EIA plates; Costar, Cambridge, MA) with a ladder of reagents as follows: first, HA molecules purified from influenza A/PR8 virus or NIBRG14; second, nasal washings, bronchoalveolar washings, or serum; third, either goat anti-mouse IgA antibody (α-chain specific; Amersham Biosciences, Piscataway, NJ) or goat anti-mouse IgG antibody (γ-chain-specific; Amersham Biosciences) conjugated with biotin; fourth, streptavidin conjugated with alkaline phosphatase (Life Technologies, Rockville, MD); and fifth, *p*-nitrophenylphosphate. The amount of chromogen produced was determined by measuring the absorbance at 405 nm using an ELISA reader. A twofold serial dilution of either purified A/PR8 HA-specific IgA (320 ng/ml) or A/PR8 HA-specific monoclonal IgG (160 ng/ml) was used as a standard, as described previously [Asahi et al., 2002]. The binding kinetics of the standard A/PR8 HA-specific monoclonal IgG was comparable with A/PR8 HA-specific IgG obtained from immunized mice. The A/PR8 HA-specific antibody concentration of each sample was determined from standard regression curves constructed for each assay with a programmed SJeia Autoreader (Model ER-8000; Sanko Junyaku, Tokyo, Japan). Standards for NIBRG14-reactive IgA and IgG antibody titration were prepared from the nasal washings or serum of survived mice after H5N1 virus challenge, and expressed using the same arbitrary units (160-unit). The NIBRG14-reactive antibody titer of each sample was determined from the standard regression curve constructed by twofold serial dilution of the 160-unit standard for each assay.

Before the hemagglutination inhibition tests, receptor-destroying enzyme (RDE II; Denka Seiken Co., Ltd, Tokyo, Japan) was added to the RBC-treated sera at 37°C overnight to inactivate non-specific hemagglutination inhibitors, followed by incubation at 56°C for 1 hr to inactivate RDE. Briefly, hemagglutination inhibition tests were performed by mixing 25 μl aliquots of serial twofold dilutions of the treated serum samples with four HA units of virus in microtiter plates and incubating them at room temperature for 30 min. Then, 50 μl of 0.5% chicken RBCs were added to each well and incubated at room temperature for 30–40 min. The hemagglutination inhibition titer was expressed as the reciprocal of the highest serum dilution that completely inhibited hemagglutination of four HA units of the virus.

The virus titer was measured as follows: 200 μl aliquots of serial 10-fold dilutions of the nasal washings were inoculated into MDCK cells in six-well plates. After incubation for 1 hr, each well was overlaid with 2 ml of agar medium. The number of plaques in each well was counted 2 days after inoculation. All experiments were repeated independently at least three times, and the data are presented as means ± SD.

Antigen-Specific T-Cell Response

Antigen-specific T-cell responses were measured as described previously [Ichinohe et al., 2005]. Spleens were harvested from mice 1 week after booster vaccination. After preparation of a single-cell suspension, T-cells were purified by depletion of $CD11b^+$ (Mac-1), $CD45R^+$ (B220), $DX5^+$, and $Ter\text{-}119^+$ cells using a magnetic cell sorter (MACS: Militenyi Biotec, Bergisch, Germany). To prepare antigen-presenting cells, splenocytes from normal BALB/c mice were depleted of

CD90 (Thy1.2)$^+$ cells by MACS and irradiated at 2,000 cGy.

T-cells were purified from the spleen (1×10^5 cells/well) and cultured with irradiated antigen-presenting cells (5×10^5 cells/well) in the presence or absence of A/PR8 vaccine (0.1, 1, or 10 μg/ml). After 4 days of culture, the cytokine concentration in the culture supernatant was measured by ELISA using a Mouse interferon-γ Immunoassay Kit (Biosource International, Camarillo, CA) according to the manufacturer's instructions.

Bone Marrow-Derived Dendritic Cell Preparation and Mycelial Extract Sensitivity Analysis

Bone marrow cells were isolated from the femurs and tibiae of wild-type or MyD88-deficient mice and bone marrow-derived dendritic cells were prepared as described [Inaba et al., 1992]. Lipopolysaccharide (1 μg/ml), Zymosan (2 μg/ml), *P. linteus* (5 μg/ml), *M. gracilenta* (5 μg/ml), *L. edodes* (5 μg/ml), or *G. frondosa* (5 μg/ml) was added on day 5 after cultivation with granulocyte–macrophage colony stimulating factor (Wako, Tokyo, Japan). On day 6, culture supernatants were collected for tumor necrosis factor (TNF)-α titration. Concentrations of TNF-α were determined by ELISA using a Mouse TNF-α Immunoassay Kit (Biosource International) according to the manufacturer's instructions.

Statistical Analysis

Comparisons between experimental groups were performed by Student's *t*-test. $P < 0.05$ was considered significant.

RESULTS

Local and Systemic Antibody Responses in BALB/c Mice Immunized Intranasally With the Hemagglutinin Vaccine and Mycelia Extracts as Adjuvants

The immune-enhancing effects of 12 varieties of mycelia extracts as mucosal adjuvants for intranasal influenza vaccine were investigated in BALB/c mice (Fig. 1). The mice were immunized twice intranasally with 1 μg of HA vaccine in combination with various adjuvants and the activities of the mycelial extracts were compared. Mice treated with mycelia extracts from *P. linteus*, *M. gracilenta*, *G. frondosa*, and *L. edodes*-adjuvanted vaccines developed sufficient levels of both HA-specific IgAs in the nasal washings and IgGs in the serum (Fig. 1). No specific antibodies were detected in the nasal washings or serum from control mice immunized with non-adjuvanted vaccine (Fig. 1).

Intranasal Immunization With the Hemagglutinin Vaccine Combined With Mycelia Extracts Protects Against Lethal Influenza Virus Lung Infection in Mice

Next, the protective effects of intranasal immunization with HA vaccine combined with mycelia extracts against lethal influenza virus lung infection were examined (Fig. 2). Mice immunized with *P. linteus*-adjuvanted vaccine showed equivalent amounts of IgG in the lung washings and serum when compared with those immunized with poly(I:C)-adjuvanted vaccine, and the viral titer of the lung washings was remarkably decreased compared with that of the control group (Fig. 2A). *M. gracilenta*- or *L. edodes*-adjuvanted

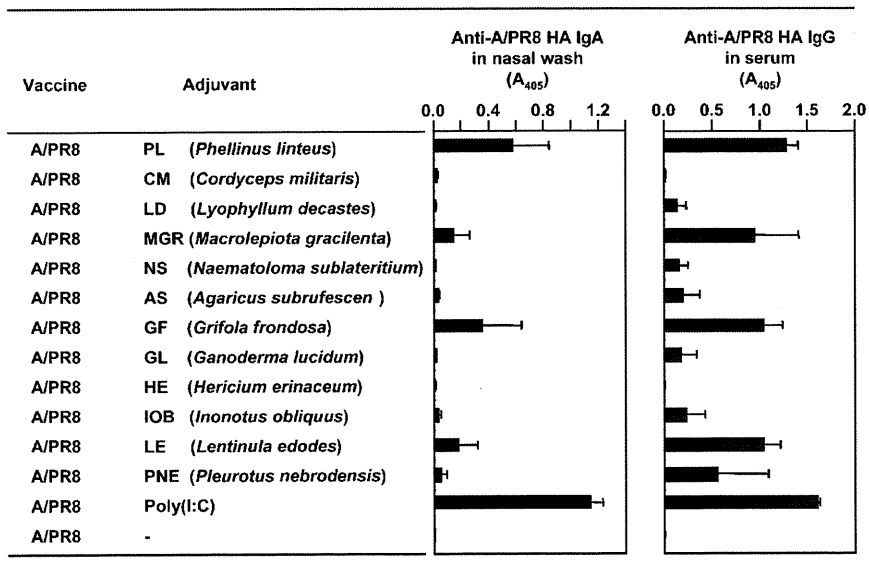

Fig. 1. Anti-A/PR8 hemagglutinin-specific IgA and IgG responses in BALB/c mice immunized intranasally with hemagglutinin vaccine alone, or in combination with various mycelia extracts or poly(I:C). Nasal washings and serum samples were collected 14 days after the final immunization. Antibody titers were measured by ELISA. Data represent the means ± SE of three mice per group.

vaccines conferred a partial but significant reduction in lung wash virus titers (Fig. 2A), while the virus titer in the lung washings of mice immunized with *G. frondosa*-adjuvanted vaccine was not altered compared to that of the control mice (Fig. 2A). The hemagglutination inhibition titer from each group corresponded with the IgG titer in lung washings and serum (Fig. 2A).

To examine the protective effects of these mycelia extract-adjuvanted vaccines against lethal influenza virus challenge, mice were inoculated with a lethal dose (40 LD_{50}) of influenza A/PR8 virus (Fig. 2B). Mice that had been immunized previously with *P. linteus*- or poly(I:C)-adjuvanted vaccine exhibited no remarkable change in body weight 14 days after virus challenge. In mice that had been immunized with vaccine adjuvanted with mycelia extracts from *M. gracilenta*, *G. frondosa*, or *L. edode*, body weights decreased gradually until day 6 after virus challenge, and then recovered from days 7 to 14 (Fig. 2B). Control mice that had been immunized with non-adjuvanted vaccine suffered from marked loss of body weight. The survival rate of mice immunized with *P. linteus*-adjuvanted vaccine was 100% at 14 days after virus challenge, suggesting that *P. linteus*-adjuvanted vaccine protected the mice against lethal lung infection as effectively as vaccine containing the poly(I:C) adjuvant (Fig. 2B). Meanwhile, the survival rates of mice immunized with vaccines adjuvanted with mycelial extracts from *M. gracilenta*, *G. frondosa*, or *L. edode* ranged from 40% to 60% at day 14 after lethal lung infection (Fig. 2B). All mice immunized with non-adjuvanted vaccine were deceased by 7 days after challenge.

Intranasal Administration of *Phellinus linteus*-Adjuvanted H5N1 Vaccine Protects Mice From Highly Pathogenic H5N1 Influenza Virus Variant Challenge

Next, the efficacy of *P. linteus*-adjuvanted vaccine against homologous (A/Vietnam/1194/2004) and heterologous (A/Indonesia/6/2005) H5N1 influenza virus challenge was examined in BALB/c mice (Fig. 3). The mice were immunized twice intranasally with 1 μg of formalin-inactivated whole H5N1 virus vaccine (NIBRG14) alone, or in combination with 500 μg of *P. linteus* extract. At 2 weeks after the final immunization, the mice were challenged by intranasal administration of 1,000 PFU of H5N1 influenza viruses.

The concentrations of anti-NIBRG14 IgA and IgG antibodies in nasal washings and serum, respectively, were much higher in animals immunized intranasally with *P. linteus*-adjuvanted NIBRG14 vaccine than in mice immunized with the vaccine alone or in non-immunized mice (Fig. 3A). In response to homologous viral challenge (A/Vietnam/1194/2004), the mice immunized with *P. linteus*-adjuvanted vaccine showed a significant reduction in virus titer compared with control mice (Fig. 3A). The mice vaccinated with *P. linteus*-adjuvanted vaccine survived longer than 14 days post-infection, while the mice immunized with

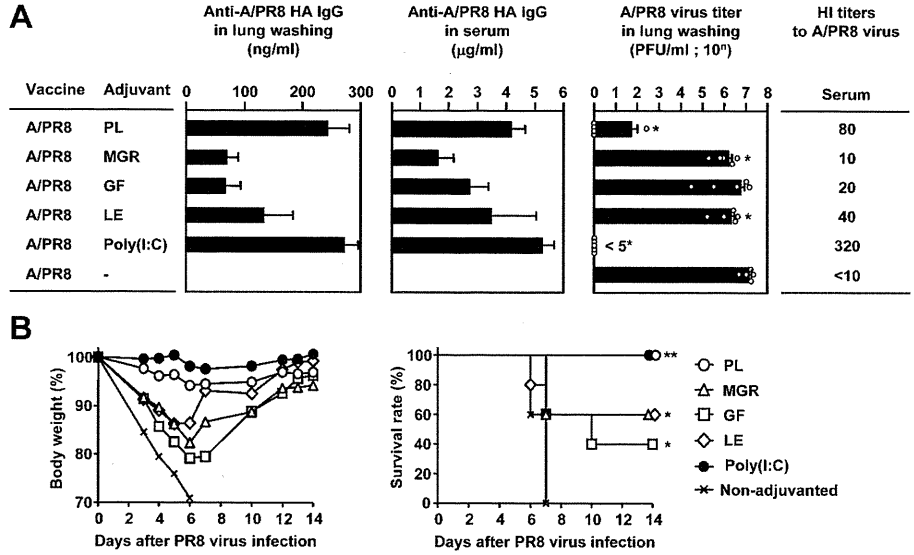

Fig. 2. **A**: Anti-A/PR8 hemagglutinin-specific IgG antibodies in lung washings and serum, and A/PR8 virus titer in lung washings. The mice were immunized twice intranasally with 1 μg of hemagglutinin vaccine alone, or in combination with extracts of mycelia from *P. linteus* (PL), *Macrolepiota gracilenta* (MGR), *Grifola frondosa* (GF), *L. edodes* (LE), or poly(I:C). Two weeks after the final immunization, the immunized mice were challenged by administration of 1,000 PFU (40 LD_{50}) of A/PR8 influenza viruses into the lung, and samples were collected 3 days after the challenge. The concentrations of IgG antibodies and virus titers from five mice from each group were measured by ELISA and plaque assay using MDCK cells, respectively. Each column represents the mean ± SE of five mice per group and open circles indicate individual animals. The virus titers were statistically compared to those of non-adjuvanted mice ($^*P < 0.05$). The hemagglutination inhibition (HI) titers against homologous A/PR8 influenza virus in the serum were measured at 2 weeks after the final immunization. The data are presented per group, and expressed as reciprocals of the highest dilution that completely inhibits hemagglutination of four HA units of the virus. **B**: Body weight and survival curves of the immunized mice after lethal A/PR8 virus challenge. Each point represents the ratio relative to the initial body weight (average) of five mice for each day after challenge (left panel). The survival rates were monitored for 14 days (right panel). $^{**}P < 0.01$ versus control mice, log-rank test.

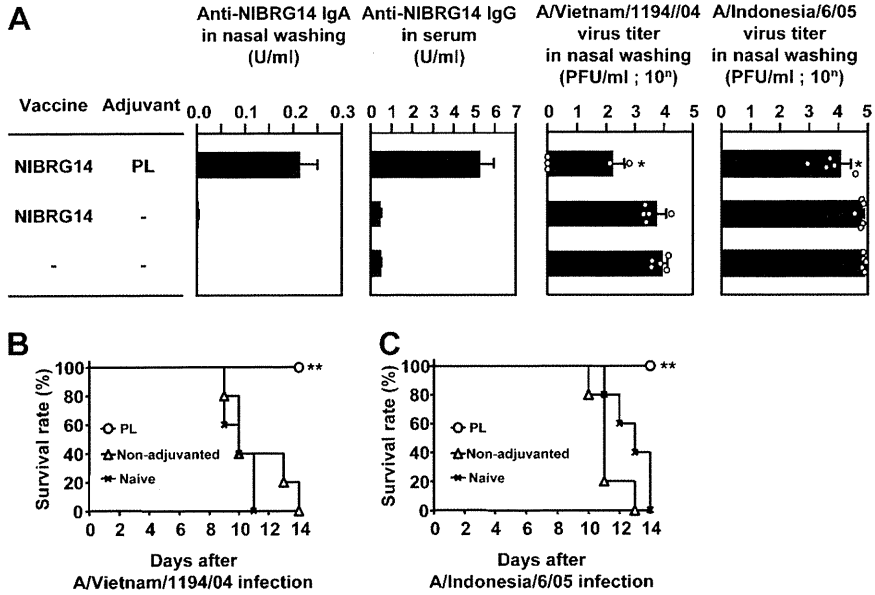

Fig. 3. Anti-NIBRG14-specific IgA and IgG responses, and H5N1 virus titers in nasal washings and survival rates after lethal challenge with homologous influenza A/Vietnam/1194/04 and heterologous influenza A/Indonesia/6/05 viruses. **A**: Anti-NIBRG14-specific IgA and IgG responses and H5N1 virus titer in the nasal washings. The mice were immunized twice intranasally with vaccine alone, or in combination with mycelia extracts of *Phellinus linteus* (PL), then challenged by intranasal administration of 1,000 PFU of influenza A/Vietnam/1194/04 or influenza A/Indonesia/6/05 virus 14 days after the final immunization. Nasal washings and serum samples were collected 3 days after the challenge. The concentrations of IgA and IgG antibodies and virus titers from five mice from each group were measured by ELISA and plaque assay using MDCK cells, respectively. Each column represents the mean values ± SE of five mice per group, and open circles indicate individual animals. The virus titers were statistically compared to those of non-immunized mice ($^*P < 0.05$). (**B**,**C**) The survival curves of mice immunized according to the same schedule as in Figure 2A after lethal influenza A/Vietnam/1194/04 (B) or influenza A/Indonesia/6/05 (C) virus challenge is depicted. The survival rates were monitored for 14 days. $^{**}P < 0.01$ versus control mice, log-rank test.

non-adjuvanted vaccine or non-immunized mice succumbed to disease by days 14 and 11, respectively (Fig. 3B). In the group challenged with heterologous A/Indonesia/6/2005 virus, mice immunized with *P. linteus*-adjuvanted vaccine showed a significant reduction in virus titer compared to the control mice (Fig. 3A) and survived longer than 14 days post-infection (Fig. 3C), while none of the mice immunized with non-adjuvanted vaccine or non-immunized mice survived more than 14 days post-infection (Fig. 3C). None of the surviving mice exhibited any clinical signs of infection, such as ruffled hair or emaciation, following the virus challenge. These results clearly indicate that intranasal administration of H5N1 vaccine in combination with *P. linteus* extract protects mice against highly pathogenic homologous and heterologous influenza A virus H5N1 infection.

Intranasal Immunization With the Hemagglutinin Vaccine With Mycelia Extract Induces a Weak Systemic T-Cell Response

To examine whether intranasal administration of influenza vaccine induces a T-cell response, levels of interferon-γ were measured in supernatants of T-cells from spleen and cervical lymph nodes of immunized mice in co-culture with antigen-presenting cells and PR8 vaccine (Fig. 4). Briefly, T-cells isolated from the spleen or cervical lymph nodes of mice 7 days after the final immunization were cultured with irradiated antigen-presenting cells in the presence or absence of A/PR8 vaccine at 0.1, 1.0 or 10 μg/ml. Low but significant levels of interferon-γ were detected in the splenic T-cells of mice immunized with *P. linteus*-adjuvanted vaccine (Fig. 4A). However, there was no significant effect on interferon-γ production in splenic T-cells of mice immunized by A/PR8 vaccine adjuvanted with *M. gracilenta*, *G. frondosa*, or *L. edode* mycelial extracts. Similarly, *P. linteus*-adjuvanted vaccine induced little T-cell response in cervical lymph nodes (Fig. 4B). These results suggest that immunization with a combination of vaccine and mycelia extract induces a relatively weak T-cell response.

MyD88 Participates in Mycelia Extract Stimulated Production of Proinflammatory Cytokines in Bone Marrow-Derived Dendritic Cells

Crude mycelia extract contains proteoglycans, hemicellulase, and β-glucans [Ukawa et al., 2000] and activates innate immune responses via CD14/TLR4 or dectin-1 (a β-glucan-specific C-type lectin receptor)-dependent pathways [Saijo et al., 2007; Taylor et al., 2007]. Because MyD88 is a general adaptor/regulator molecule for the Toll/IL-1R family of receptors [Medzhitov et al., 1998], cytokine production was measured in wild-type and MyD88-deficient bone marrow-derived dendritic cells following stimulation with mycelia extract. Bone marrow-derived dendritic

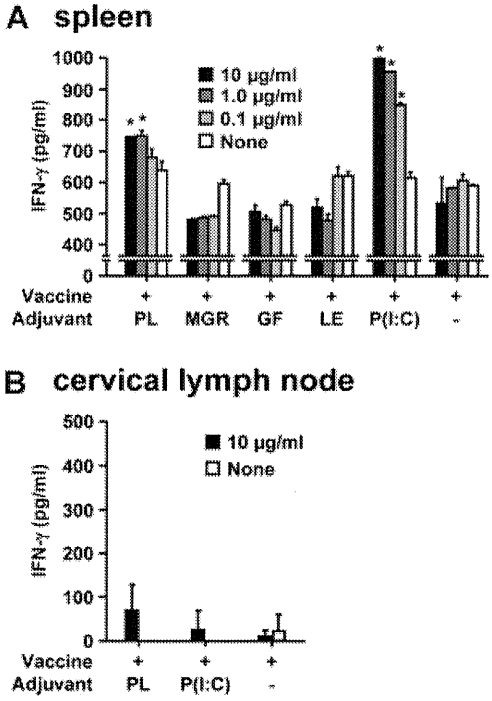

Fig. 4. In vitro responses of influenza A/PR8 virus-specific T-cells derived from mice immunized intranasally with hemagglutinin vaccine alone, or in combination with various mycelial extracts or poly(I:C). Spleens (**A**) and cervical lymph nodes (**B**) were isolated 1 week after the final immunization and re-stimulated with T-cell-depleted splenocytes that had been pulsed with the indicated concentration of A/PR8 hemagglutinin vaccine. Production of interferon-γ in the culture supernatant was measured by ELISA at 4 days after the antigen re-stimulation. These results are presented as the means of two independent experiments. $^*P < 0.05$ versus non-stimulated sample.

cells from wild-type or MyD88-deficient mice were stimulated with lipopolysaccharide, Zymosan, or mycelia extracts in vitro for 24 hr, and their ability to secrete TNF-α was examined. After stimulation with Zymosan, *P. linteus*, *M. gracilenta*, *G. frondosa*, or *L. edode* extracts, TNF-α production was partially but significantly reduced in MyD88-deficient dendritic cells in comparison to wild-type dendritic cells, and was drastically reduced after lipopolysaccharide stimulation in MyD88-deficient dendritic cells as compared to wild-type (Fig. 5). All mycelia extracts strongly induced TNF-α and IL-6 as much as stimulation with lipopolysaccharide or Zymosan in bone marrow-derived dendritic cells, but not IL-12 or p70. In addition, while lipopolysaccharide and Zymosan strongly enhanced CD40 expression in dendritic cells, treatment with mycelial extracts from *P. linteus*, *M. gracilenta*, *G. frondosa*, or *L. edode* only modestly enhanced CD40 expression in dendritic cells. These results indicate that proinflammatory cytokine production in bone marrow-derived dendritic cells in response to stimulation by mycelial extracts is partly dependent on MyD88 and that the adjuvant activity of mycelia extracts may be achieved through activation of dendritic cells.

DISCUSSION

The results of the present study clearly demonstrate that extracts of mycelia from edible mushrooms, especially *P. linteus*, are an effective mucosal adjuvant when administered intranasally with influenza vaccine. Nasal immunization induced not only an increase in mucosal secretory IgA, but also a high titer of anti-HA IgG in the serum. This immune reaction resulted

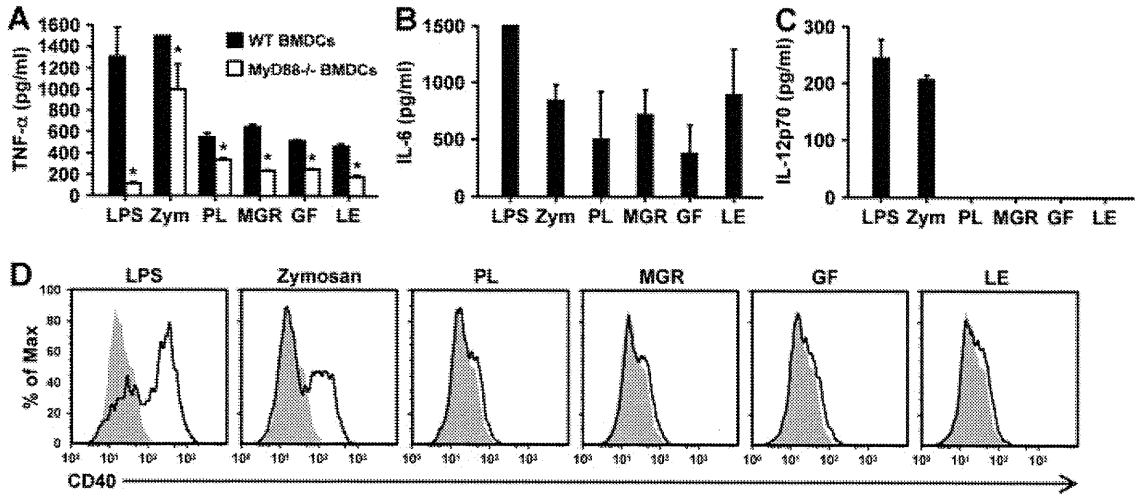

Fig. 5. Tumor necrosis factor (TNF)-α (**A**), IL-6 (**B**), and IL-12p70 production from bone marrow-derived dendritic cells (BMDCs). BMDCs (5×10^5 cells/well) from wild-type (filled columns) or MyD88-deficient mice (open columns) were stimulated with lipopolysaccharide (LPS), Zymosan (Zym.), *Phellinus linteus* (PL), *Macrolepiota gracilenta* (MGR), *Grifola frondosa* (GF), or *Lentinula edodes* (LE) for 24 hr as described in Materials and Methods Section. The culture supernatants were collected and the concentration of TNF-α (A), IL-6 (B) and IL-12p70 (**C**) were measured by ELISA. Data represent the means ± SD of duplicate samples. $^*P < 0.05$, wild-type versus MyD88-deficient dendritic cells. The expression of the co-stimulatory molecule CD40 was measured by flow cytometry after 24 h of stimulation (**D**). The gray histograms show the expressions on the unstimulated cells, and the bold lines show the expression of CD40.

in cross-protective immune responses against both homologous and heterologous influenza variants, including highly pathogenic H5N1 influenza virus isolates. Administration of the formalin-inactivated whole H5N1 vaccine (NIBRG14) or the PR8 HA vaccine combined with *P. linteus* extract following a two-dose immunization protocol was able to confer protection against infection with lethal influenza A/Vietnam/1194/2004 (H5N1) virus, influenza A/Indonesia/6/2005 (H5N1) virus, and lethal lung infection (40 LD_{50}) by PR8 influenza virus, respectively. These results indicate that *P. linteus* extract is an effective mucosal adjuvant when administered intranasally with influenza vaccine. The *P. linteus*-adjuvanted vaccines induced poor T-cell responses, indicating that cross-protection may be mediated primarily by the mucosal immune response, probably via the activity of secretory IgA antibodies against viral proteins. It has been shown that polymeric immunoglobulin receptor-knockout mice do not secrete IgA and exhibit less cross-protective efficacy against variant influenza virus infection [Asahi et al., 2002]. Although neutralizing activity against heterologous A/Vietnam/1194/2004 (H5N1) virus was not detected in the nasal washings, this was likely due to dilution with PBS when the nasal washings were collected. The concentration of vaccine-specific IgA in the nasal wash samples was much lower than the physiological concentration in the nasal mucosa, and therefore neutralizing activity in the nasal washings may not have been detectable.

Intranasal vaccination is advantageous for protection against influenza virus infection due to the induction of secretory IgA at the mucosal surface, which elicits a more effective cross-protective immunity compared to serum IgG. In fact, the cross-protective effects of *P. linteus*-adjuvanted vaccine were observed even against virulent heterologous H5N1 variants. Antigen-specific T-cell responses were weak in mice that had been immunized intranasally with vaccine and mycelia extracts from *P. linteus*, indicating that homologous and heterologous protection is primarily accomplished by secretory IgA at the mucosal surface.

Although mycelia extracts did not activate dendritic cells to the same extent as lipopolysaccharide or Zymosan, they induced high levels of cytokines such as TNF-α and IL-6 as much as stimulation with lipopolysaccharide or Zymosan. It has been shown that dectin-1 mediates the phagocytosis of β-glucan-bearing ligands, including yeast-derived particles such as Zymosan [Herre et al., 2004]. The phagocytosis of pathogens is a critical host defence mechanism, not only for clearance of the invading microorganism, but also for the generation of antigenic fragments for presentation to $CD4^+$ T-cells to induce a subsequent adaptive immune response [Dzionek et al., 2001]. Toll-like receptors 3, 7, 8, and 9 are localized to intracellular compartments and specialize in recognition of viral nucleic acids in the endosome [Iwasaki and Medzhitov, 2004]. In this regard, concomitant administration of mycelial extracts and a toll-like receptor agonist, such as synthetic double-stranded RNA poly(I:C), synthetic imidazoquinoline compounds, or oligodeoxynucleotides containing cytosine–guanine motifs may be more effective than either mycelial extracts or toll-like receptor agonists alone, by reason of accumulation of vaccine with a toll-like receptor agonist into endosomal compartments that express toll-like receptors 3, 7, 8, and 9. In fact, complexing toll-like receptor 3 or 9 agonists to cationic liposomes markedly potentiated their ability to activate immune responses [Zaks et al., 2006]. These synergistic effects may contribute to the enhancement of mucosal adjuvant effects, leading to complete protection against viral challenge.

A major objective of intranasal influenza vaccine development is the design of an adjuvant that can provide effective mucosal immune activity and at the same time is stable and safe for clinical application in humans. Although poly(I:C) is a potent mucosal adjuvant, it has been associated with some adverse events during clinical trials of intravenous administration. Poly(I:C) induced a number of side effects in humans, including renal failure and hypersensitivity, in a previous clinical trial using dosages as high as 75 mg of poly(I:C)/m^2 at day 0 followed by daily administration from day 7 to a maximum of 35 days [Robinson et al., 1976]. Although the crude mycelia extracts used in the present study are not as effective as poly(I:C) as an adjuvant, identification of the active ingredients has the potential to produce an adjuvant as effective as poly(I:C). The mycelial extracts are derived from edible mushrooms and are separated by boiling, indicating that the active ingredients in the adjuvant are thermotolerant, whereas poly(I:C) loses adjuvant activity after boiling at 95°C for 5 min [Ichinohe et al., 2005]. It has also been shown that oral administration of mushroom extracts decreases IgE levels by modulation of Th1/Th2 balance. Inagaki et al. [2005] reported that oral administration of *P. linteus* significantly inhibited the IgE-dependent mouse triphasic cutaneous reaction, and Lim et al. [2005] demonstrated that *P. linteus* given orally decreased IgE concentration in serum and murine mesenteric lymph node lymphocytes, and increased concanavalin A-induced interferon-γ secretion in mesenteric lymphocytes. These characteristics offer great advantages for clinical application.

For the clinical application, we need to evaluate the effective dose of vaccine in human trials. The effectiveness of intranasal vaccine with injection dose (15 μg) in humans could be roughly assessed by the ability of ~0.1 μg vaccine to induce an immune response to provide protection against infection in BALB/c mice immunized intranasally according to a two-dose regimen [Tamura et al., 2005]. These data suggest that the vaccine dose in BALB/c mice in the current study (1 μg of vaccine per mouse) corresponded to ~10 times the dose in subcutaneous injection in human. Identification of the active ingredients in the crude mycelial extracts could reduce the doses. Further investigation is necessary to identify the active ingredients to produce more potent mucosal adjuvant.

In summary, intranasal immunization with influenza vaccine and extract of mycelia from *P. linteus*-induced cross-protective mucosal immunity against heterologous H5N1 influenza viruses in mice. Intranasal immunization with influenza vaccine containing *P. linteus* extract may thus represent a strategy to generate protective mucosal immunity in humans against newly emerging and highly pathogenic avian influenza viruses. Because prophylactic agents, including vaccines, must ensure sufficient safety for clinical use, further studies are required to determine whether such a nasal vaccine would be effective for use in humans.

ACKNOWLEDGMENTS

The authors are deeply grateful to Dr. Wilina Lim (Department of Health, the government of Hong Kong) for providing us influenza A virus A/Vietnam/1194/2004 (H5N1), Dr. T. Tanaka (Toray Industries, Inc., Kamakura, Kanagawa, Japan) for providing the poly(I:C), Dr. U. Suzuki (Kitasato Institute, Saitama, Japan) for providing us the vaccines, and Dr. S. Nagasaka (Tokyo University of Science, Chiba, Japan) for technical advice.

REFERENCES

Adachi O, Kawai T, Takeda K, Matsumoto M, Tsutsui H, Sakagami M, Nakanishi K, Akira S. 1998. Targeted disruption of the MyD88 gene results in loss of IL-1- and IL-18-mediated function. Immunity 9:143–150.

Asahi Y, Yoshikawa T, Watanabe I, Iwasaki T, Hasegawa H, Sato Y, Shimada S, Nanno M, Matsuoka Y, Ohwaki M, Iwakura Y, Suzuki Y, Aizawa C, Sata T, Kurata T, Tamura S. 2002. Protection against influenza virus infection in polymeric Ig receptor knockout mice immunized intranasally with adjuvant-combined vaccines. J Immunol 168:2930–2938.

Asahi-Ozaki Y, Itamura S, Ichinohe T, Strong P, Tamura S, Takahashi H, Sawa H, Moriyama M, Tashiro M, Sata T, Kurata T, Hasegawa H. 2006. Intranasal administration of adjuvant-combined recombinant influenza virus HA vaccine protects mice from the lethal H5N1 virus infection. Microbes Infect 8:2706–2714.

Bernardshaw S, Hetland G, Grinde B, Johnson E. 2006. An extract of the mushroom Agaricus blazei Murill protects against lethal septicemia in a mouse model of fecal peritonitis. Shock 25:420–425.

Coulter A, Harris R, Davis R, Drane D, Cox J, Ryan D, Sutton P, Rockman S, Pearse M. 2003. Intranasal vaccination with ISCOMATRIX adjuvanted influenza vaccine. Vaccine 21:946–949.

Dzionek A, Sohma Y, Nagafune J, Cella M, Colonna M, Facchetti F, Gunther G, Johnston I, Lanzavecchia A, Nagasaka T, Okada T, Vermi W, Winkels G, Yamamoto T, Zysk M, Yamaguchi Y, Schmitz J. 2001. BDCA-2, a novel plasmacytoid dendritic cell-specific type II C-type lectin, mediates antigen capture and is a potent inhibitor of interferon alpha/beta induction. J Exp Med 194:1823–1834.

Gao P, Watanabe S, Ito T, Goto H, Wells K, McGregor M, Cooley AJ, Kawaoka Y. 1999. Biological heterogeneity, including systemic replication in mice, of H5N1 influenza A virus isolates from humans in Hong Kong. J Virol 73:3184–3189.

Hasegawa H, Ichinohe T, Strong P, Watanabe I, Ito S, Tamura S, Takahashi H, Sawa H, Chiba J, Kurata T, Sata T. 2005. Protection against influenza virus infection by intranasal administration of hemagglutinin vaccine with chitin microparticles as an adjuvant. J Med Virol 75:130–136.

Herre J, Marshall AS, Caron E, Edwards AD, Williams DL, Schweighoffer E, Tybulewicz V, Reis e Sousa C, Gordon S, Brown GD. 2004. Dectin-1 uses novel mechanisms for yeast phagocytosis in macrophages. Blood 104:4038–4045.

Ichinohe T, Watanabe I, Ito S, Fujii H, Moriyama M, Tamura S, Takahashi H, Sawa H, Chiba J, Kurata T, Sata T, Hasegawa H. 2005. Synthetic double-stranded RNA Poly(I:C) combined with mucosal vaccine protects against influenza virus infection. J Virol 79:2910–2919.

Ichinohe T, Watanabe I, Tao E, Ito S, Kawaguchi A, Tamura S, Takahashi H, Sawa H, Moriyama M, Chiba J, Komase K, Suzuki Y, Kurata T, Sata T, Hasegawa H. 2006. Protection against influenza virus infection by intranasal vaccine with surf clam microparticles (SMP) as an adjuvant. J Med Virol 78:954–963.

Ichinohe T, Kawaguchi A, Tamura S, Takahashi H, Sawa H, Ninomiya A, Imai M, Itamura S, Odagiri T, Tashiro M, Chiba J, Sata T, Kurata T, Hasegawa H. 2007a. Intranasal immunization with H5N1 vaccine plus Poly I:Poly C(12)U, a Toll-like receptor agonist, protects mice against homologous and heterologous virus challenge. Microbes Infect (Institut Pasteur) 9:1333–1340.

Ichinohe T, Tamura S, Kawaguchi A, Ninomiya A, Imai M, Itamura S, Odagiri T, Tashiro M, Takahashi H, Sawa H, Mitchell WM, Strayer DR, Carter WA, Chiba J, Kurata T, Sata T, Hasegawa H. 2007b. Cross-protection against H5N1 influenza virus infection is afforded by intranasal inoculation with seasonal trivalent inactivated influenza vaccine. J Infect Dis 196:1313–1320.

Ichinohe T, Iwasaki A, Hasegawa H. 2008. Innate sensors of influenza virus: Clues to developing better intranasal vaccines. Expert Rev Vaccines 7:1435–1445.

Inaba K, Inaba M, Romani N, Aya H, Deguchi M, Ikehara S, Muramatsu S, Steinman RM. 1992. Generation of large numbers of dendritic cells from mouse bone marrow cultures supplemented with granulocyte/macrophage colony-stimulating factor. J Exp Med 176:1693–1702.

Inagaki N, Shibata T, Itoh T, Suzuki T, Tanaka H, Nakamura T, Akiyama Y, Kawagishi H, Nagai H. 2005. Inhibition of IgE-dependent mouse triphasic cutaneous reaction by a boiling water fraction separated from mycelium of Phellinus linteus. Evid Based Complement Altern Med 2:369–374.

Iwasaki A, Medzhitov R. 2004. Toll-like receptor control of the adaptive immune responses. Nat Immunol 5:987–995.

Kim GY, Park SK, Lee MK, Lee SH, Oh YH, Kwak JY, Yoon S, Lee JD, Park YM. 2003. Proteoglycan isolated from Phellinus linteus activates murine B lymphocytes via protein kinase C and protein tyrosine kinase. Int Immunopharmacol 3:1281–1292.

Kim GY, Ko WS, Lee JY, Lee JO, Ryu CH, Choi BT, Park YM, Jeong YK, Lee KJ, Choi KS, Heo MS, Choi YH. 2006. Water extract of Cordyceps militaris enhances maturation of murine bone marrow-derived dendritic cells in vitro. Biol Pharm Bull 29:354–360.

Kodama N, Asakawa A, Inui A, Masuda Y, Nanba H. 2005. Enhancement of cytotoxicity of NK cells by D-Fraction, a polysaccharide from Grifola frondosa. Oncol Rep 13:497–502.

Kuo MC, Weng CY, Ha CL, Wu MJ. 2006. Ganoderma lucidum mycelia enhance innate immunity by activating NF-kappaB. J Ethnopharmacol 103:217–222.

Lim BO, Jeon TI, Hwang SG, Moon JH, Park DK. 2005. Phellinus linteus grown on germinated brown rice suppresses IgE production by the modulation of Th1/Th2 balance in murine mesenteric lymph node lymphocytes. Biotechnol Lett 27:613–617.

Medzhitov R, Preston-Hurlburt P, Kopp E, Stadlen A, Chen C, Ghosh S, Janeway CA, Jr. 1998. MyD88 is an adaptor protein in the hToll/IL-1 receptor family signaling pathways. Mol cell 2:253–258.

Mutsch M, Zhou W, Rhodes P, Bopp M, Chen RT, Linder T, Spyr C, Steffen R. 2004. Use of the inactivated intranasal influenza vaccine and the risk of Bell's palsy in Switzerland. N Engl J Med 350:896–903.

Nicolson C, Major D, Wood JM, Robertson JS. 2005. Generation of influenza vaccine viruses on Vero cells by reverse genetics: An H5N1 candidate vaccine strain produced under a quality system. Vaccine 23:2943–2952.

Robinson RA, DeVita VT, Levy HB, Baron S, Hubbard SP, Levine AS. 1976. A phase I-II trial of multiple-dose polyriboinosic-polyribocytidylic acid in patieonts with leukemia or solid tumors. J Natl Cancer Inst 57:599–602.

Saijo S, Fujikado N, Furuta T, Chung SH, Kotaki H, Seki K, Sudo K, Akira S, Adachi Y, Ohno N, Kinjo T, Nakamura K, Kawakami K, Iwakura Y. 2007. Dectin-1 is required for host defense against Pneumocystis carinii but not against Candida albicans. Nat Immunol 8:39–46.

Sanzen I, Imanishi N, Takamatsu N, Konosu S, Mantani N, Terasawa K, Tazawa K, Odaira Y, Watanabe M, Takeyama M, Ochiai H. 2001. Nitric oxide-mediated antitumor activity induced by the extract from Grifola frondosa (Maitake mushroom) in a macrophage cell line, RAW264.7. J Exp Clin Cancer Res 20:591–597.

Sorimachi K, Akimoto K, Ikehara Y, Inafuku K, Okubo A, Yamazaki S. 2001. Secretion of TNF-alpha, IL-8 and nitric oxide by macrophages activated with Agaricus blazei Murill fractions in vitro. Cell Struct Funct 26:103–108.

Tamura S, Tanimoto T, Kurata T. 2005. Mechanisms of broad cross-protection provided by influenza virus infection and their application to vaccines. Jpn J Infect Dis 58:195–207.

Taylor PR, Tsoni SV, Willment JA, Dennehy KM, Rosas M, Findon H, Haynes K, Steele C, Botto M, Gordon S, Brown GD. 2007. Dectin-1 is required for beta-glucan recognition and control of fungal infection. Nat Immunol 8:31–38.

Ukawa Y, Ito H, Hisamatsu M. 2000. Antitumor effects of (1 → 3)-beta-D-glucan and (1 → 6)-beta-D-glucan purified from newly cultivated mushroom, Hatakeshimeji (Lyophyllum decastes Sing.). J Biosci Bioeng 90:98–104.

Zaks K, Jordan M, Guth A, Sellins K, Kedl R, Izzo A, Bosio C, Dow S. 2006. Efficient immunization and cross-priming by vaccine adjuvants containing TLR3 or TLR9 agonists complexed to cationic liposomes. J Immunol 176:7335–7345.

Vaccine 28 (2010) 6588–6596

Contents lists available at ScienceDirect

Vaccine

journal homepage: www.elsevier.com/locate/vaccine

Immunogenicity and efficacy of two types of West Nile virus-like particles different in size and maturation as a second-generation vaccine candidate

Naohiro Ohtaki[a], Hidehiro Takahashi[a], Keiko Kaneko[a], Yasuyuki Gomi[b], Toyokazu Ishikawa[b], Yasushi Higashi[b], Takeshi Kurata[a], Tetsutaro Sata[a], Asato Kojima[a,*]

[a] Department of Pathology, National Institute of Infectious Diseases, Shinjuku-ku, Tokyo 162-8640, Japan
[b] Kanonji Institute, The Research Foundation for Microbial Diseases of Osaka University, Yahata-cho, Kanonji-shi, Kagawa 768-0061, Japan

ARTICLE INFO

Article history:
Received 16 March 2010
Received in revised form 14 June 2010
Accepted 18 July 2010
Available online 1 August 2010

Keywords:
West Nile vaccine
Virus-like particle
Particle size

ABSTRACT

Virus-like particles (VLPs) of flaviviruses generated from the prM and E genes are a promising vaccine candidate. We have established cell clones continuously releasing VLPs of West Nile virus (WNV) in serum-free conditions. Two types of VLPs were distinguished by sedimenting analyses in sucrose density gradients. Fast sedimenting VLPs (*F*-VLPs) were large (40–50 nm) and composed of the E and processed mature M proteins, whereas slowly sedimenting VLPs (*S*-VLPs) were small (20–30 nm) particles consisting of the E and immature prM proteins. *F*-VLPs induced higher neutralizing antibody and anti-WNV IgG titers than *S*-VLPs. Furthermore, IgG2a was dominant over IgG1 by immunization with *F*-VLPs as with whole virion-derived antigens. Mice vaccinated with a low dose (3 ng) of *F*-VLPs showed higher protective efficacy (83% survivals) against WNV infection than *S*-VLP-immune mice (17% survivals). These results indicate that *F*-VLPs more closely resemble the virions and take a better immunogenic form than *S*-VLPs as WNV vaccine candidates.

1. Introduction

West Nile virus (WNV) is a member of Japanese encephalitis virus (JEV) serocomplex of the family Flaviviridae. WNV is widely distributed in the world, whose geographic range includes North America, Africa, Europe, Middle East and West Asia [1]. WNV has caused several outbreaks of lethal encephalitis. Humans infected with WNV develop a febrile illness and the infections can result in severe meningoencephalitis, although most cases are clinically inapparent. WNV is mainly transmitted to humans by the bite of an infected mosquito. Other routes such as blood transfusion and organ transplantation also have risks of viral infection [2,3]. However, there are no vaccines available for humans to prevent WNV infection.

WNV virions are enveloped spherical particles about 50 nm in diameter that contain three structural proteins (capsid (C), membrane (M) and envelope (E)) and the RNA genome [4,5]. The E and M proteins exist as the surface glycoproteins. The E protein functions in receptor binding, membrane fusion and viral assembly. Precursor of the M protein (prM) helps proper folding of the E protein by forming prM/E heterodimers during their translation [6]. The proteolytic cleavage of prM into M by cellular protease furin and/or exposure to an acidic environment converts the immature prM/E viral particles into the mature M/E virions with a conformational change of the E and M proteins [7,8]. Co-expression of the prM and E genes without other viral genes can produce small, capsidless and noninfectious virus-like particles (VLPs) around 20–30 nm in size, which are also called recombinant subviral particles (RSPs) or extracellular particles (EPs) [9–13]. The E and prM/M proteins that constitute VLPs appear to be identical to the viral structural proteins in proteolytic processing and glycosylation, except the arrangement of the E and prM/M proteins on the surface of particles [9,12,14,15].

Neutralizing antibodies (NTAbs) are most important to prevent flavivirus infection [16–19]. Many WNV vaccines are under development for clinical use; attenuated or defective viruses [20,21], chimeric flaviviruses replaced with the WNV prM–E gene region [22,23], other viral vectors [24] or plasmid DNA [25] encoding the prM–E gene, inactivated whole virions [26] and the ectodomain [27,28] or the receptor binding domain of the E protein [29]. The primary purpose of each prophylactic WNV vaccine is to induce NTAbs that target the E protein. WNV VLPs appear to be a promising vaccine candidate, because they are produced without propagating infectious viruses in BSL-3 facilities, leading them to be safe and

* Corresponding author at: Department of Pathology, National Institute of Infectious Diseases, Toyama 1-23-1, Shinjuku-ku, Tokyo 162-8640, Japan. Tel.: +81 3 5285 1111; fax: +81 3 5285 1189.
E-mail addresses: ohtaki@nih.go.jp (N. Ohtaki), htakahas@nih.go.jp (H. Takahashi), keiko5@nih.go.jp (K. Kaneko), ygomi@mail.biken.or.jp (Y. Gomi), toishika@mail.biken.or.jp (T. Ishikawa), yhigashi@mail.biken.or.jp (Y. Higashi), tkurata@nih.go.jp (T. Kurata), tsata@nih.go.jp (T. Sata), akojima@nih.go.jp (A. Kojima).

0264-410X/$ – see front matter © 2010 Elsevier Ltd. All rights reserved.
doi:10.1016/j.vaccine.2010.07.055

cost-effective. Furthermore, VLPs are thought to be highly immunogenic due to their conformation-dependent epitopes. In order to develop VLPs as vaccines for humans in a cell culture system, however, it is important to establish a cell line stably producing VLPs from cell substrates that are well characterized and confirmed their safety. Serum-free culture conditions are also suitable to avoid biological contaminations like animal viruses.

Here, we selected a CHO cell line as a parental cell substrate for continuously producing WNV VLPs in serum-free medium, since CHO cells have been used in manufacturing biological products for human use and in continuously producing VLPs of other flaviviruses [30,31]. In this study, we have established CHO cell clones releasing VLPs of different sizes that were separated by sucrose density gradient centrifugation. These VLPs were also distinct in the maturation status revealed by the contents of the immature prM and processed mature M proteins. Interestingly, immunogenicity was related to the size and maturation of VLPs. Large (40–50 nm) mature VLPs with the size of virions induced not only higher NTAb titers than smaller (20–30 nm) immature VLPs but also IgG2a-dominant antibody responses as infectious and inactivated whole virions did. Furthermore, large VLPs exhibited more potent protection against WNV challenge than small VLPs.

2. Materials and methods

2.1. Cells and virus

CHO-K1 cells (CCL-61; American Type Culture Collection) were grown in F12K medium (Invitrogen, Grand Island, NY) supplemented with 10% fetal bovine serum (FBS; MP Biomedicals, Aurora, OH). Cells adapted to serum-free conditions and CHO-S cells (Invitrogen) were maintained in CHO-S-SFM-II (Invitrogen). Vero E6 cells were cultured in Dulbecco's modified MEM (DMEM; Invitrogen) supplemented with 10% FBS. The NY99-6922 strain of WNV [26] was propagated and titrated on Vero E6 cell monolayers.

2.2. Establishment of stable cell lines continuously expressing the WNV prM–E gene

An expression vector, pWPME12 bsr, was constructed as described previously [13,32]. It encodes cDNA for the WNV prM–E polyprotein in pCAGGS plasmid modified by the introduction with the blasticidin S (BS)-resistant gene. CHO cells were transfected with pWPME12 bsr using Fugene-6 (Roche Diagnostics, Indianapolis, IN) and cultured in growth medium. Confluent cells were subcultured in the presence of 10 μg/mL of BS (Kaken pharmaceutical, Tokyo, Japan). BS-resistant colonies were picked by a penicillin cup method and transferred to a 24-well plate. The WNV antigens secreted in the culture supernatants were screened by antigen-capture enzyme-linked immunosorbent assay (ELISA) and the best colony #22 was selected. The #22.6 clone and #22.6.6 subclone were established from #22 cells by a limiting dilution method. For the adaptation to the serum-free SFM-II medium, #22.6 (passage number 4) and #22.6.6 (passage number 3) cells in the growth medium with 10% FBS were subsequently subcultured by increasing the ratio of SFM-II to growth medium until cells were transferred into 100% SFM-II. The serum-free cell clones established at passage 26 from #22.6 and at passage 24 from #22.6.6 were designated #22.6S and #22.6.6S, respectively.

2.3. Antigen-capture ELISA

The amounts of WNV antigens were examined by sandwich ELISA where WNV-specific neutralizing monoclonal antibody (MAb) WNY-11 was used for coating plates and detecting the bound virus antigens. The amounts of the antigens were estimated using two-fold dilutions of highly purified formalin-inactivated WNV virions (protein content determined by the Lowry method: 102 μg/mL) as a reference, as described previously [13]. Similarly, flavivirus-specific 402 MAb was also used for antigen-capture ELISA [13].

2.4. Sucrose density gradient ultracentrifugation

Culture supernatants of #22.6S cells were clarified by centrifugation at 200 × *g* for 10 min, filtration though a 0.45 μm membrane (Millex; Millipore, Bedford, MA) and then centrifugation at 10,000 × *g* for 30 min. For equilibrium sedimentation analysis, culture supernatants were layered on a 10–50% (w/w) linear sucrose gradient in 50 mM Tris–HCl (pH 7.5)–150 mM NaCl (Tris-buffered saline, TBS) and centrifuged at 160,000 × *g* for 15 h at 4 °C in an SW41-Ti rotor (Beckman Coulter, Fullerton, CA). For velocity sedimentation analysis, culture supernatants were applied to a 5–20% (w/w) linear sucrose gradient and centrifuged at 160,000 × *g* for 2 h at 4 °C. When WNV antigens were preparatively collected by the velocity sedimentation, antigen-containing solutions were loaded on a 0%, 13% and 20% (w/w) discontinuous sucrose gradient. Fractions of 0.75 mL were collected from the bottom of the tubes and analyzed by antigen-capture ELISA.

2.5. Antigen preparation

Clarified #22.6S culture supernatants were precipitated with 12% polyethylene glycol 6000 (PEG6000; WAKO Pure Chemical Industries, Osaka, Japan)–0.5 M NaCl at 4 °C overnight. The precipitates were collected by centrifugation at 10,000 × *g* for 30 min and dissolved in TBS. Insoluble materials were removed by centrifugation at 10,000 × *g* for 3 min, and the supernatants were subjected to sucrose density gradient centrifugation as described above. The peak fractions determined by antigen-capture ELISA were applied to a gel-filtration column (Hiprep Sephacryl S-300 16/60; GE healthcare, Buckinghamshire, UK) and eluted with phosphate-buffered saline (PBS) containing stabilizers (2% sorbitol and 4% inositol; WAKO) and a preservative (0.005% thimerosal; MP Biomedicals). The peak fractions were examined for the amounts of the E antigen by ELISA and stored at 4 °C until immunization of mice. Protein concentrations of the WNV antigen preparations were also determined with a Lowry method kit (DC protein assay; Bio-Rad Laboratories, Hercules, CA) according to the manufacturer's instructions.

2.6. Electron microscopy

Samples in the antigen preparation steps were processed for negative staining using copper grids. The specimens were stained with sodium phosphotungstic acid and observed on an H-7650 electron microscope (Hitachi Hi-Technologies, Tokyo, Japan).

2.7. Endoglycosidase treatment, SDS-PAGE and immunoblotting

#22.6S cells expressing WNV antigens and virus-infected Vero cells were collected at 200 × *g* for 10 min and solubilized with lysis buffer (50 mM Tris–HCl (pH 7.5)–150 mM NaCl–2 mM EDTA–1% Triton X-100). WNV antigens released into culture supernatants were recovered by centrifugation at 160,000 × *g* for 18 h and lysed. The lysates were heated at 55 °C for 20 min in denaturing buffer (50 mM Tris–HCl (pH 6.8)–2% SDS–10% glycerol). The denatured aliquots were treated with 500 U of peptide N-glycosidase F (PNGase F) or 1000 U of endoglycosidase H_f (Endo H_f) (New England Biolabs, Ipswich, MA) for 3 h at 37 °C. The digested samples were analyzed by 7.5% or 12% SDS-polyacrylamide gel

electrophoresis (SDS-PAGE) and immunoblotting with rabbit anti-JEV/WNV cross-reactive serum and rabbit anti-WNV M polyclonal antibody (IMGENEX, San Diego, CA), and peroxidase-conjugated anti-rabbit IgG (Roche Diagnostics), as described previously [13]. Immunoreactive proteins were detected with Supersignal West Femto maximum sensitivity substrate (Thermo Fisher Scientific, Waltham, MA) and quantified by a LAS-3000 imaging system (Fujifilm, Tokyo, Japan).

2.8. Immunization and analyses of antibody responses

Groups of five female 4-week-old C3H/HeN mice (Japan SLC, Hamamatsu, Japan) were intraperitoneally immunized twice at 7-day intervals with #22.6S-derived VLP antigens or formalin-inactivated WNV in ELISA-normalized doses. Sera were collected at 1 week after the second immunization and heat-inactivated. Serial two-fold dilutions of pooled sera from each group were incubated with the WNV NY99-6922 strain and then inoculated on Vero E6 cell monolayers at least in triplicate as described previously [13]. The cells were fixed with 10% formalin and stained 3 or 4 days after infection. Plaque numbers were counted and NTAb titers were expressed as the maximum serum dilutions yielding a 50% reduction in the plaque number of a virus control without mouse serum ($PRNT_{50}$). Anti-WNV immunoglobulin G (IgG) titers of individual mouse sera were determined using ELISA plates coated with formalin-inactivated WNV and horseradish peroxidase-conjugated goat anti-mouse IgG (Jackson ImmunoResearch, West Grove, PA) [13]. Optical density (O.D.) cutoff values were calculated as the mean O.D. of sera from PBS-immunized mice plus 3 standard deviations. Endpoint titers were expressed as the reciprocal of the maximum dilution giving a greater O.D. value than the cutoff value. IgG1 and IgG2a titers were similarly determined by ELISA with horseradish peroxidase-conjugated goat anti-mouse IgG1 and anti-mouse IgG2a (Southern Biotechnology Associates, Birmingham, AL), respectively.

2.9. Protection of vaccinated mice against lethal WNV challenge

Groups of mice were immunized twice as described above. At 1 week after the second immunization they were challenged by intraperitoneal injection with 10^3 pfu of the NY99-6922 strain of WNV. The challenged mice were observed daily for 14 days.

3. Results

3.1. Establishment of CHO cell clones stably producing prM/M and E antigens

CHO cells were obtained from ATCC to establish stable cells expressing WNV VLPs. The CHO cells were transfected with pWPME12 bsr that was previously constructed for the most efficient expression of the WNV prM/M and E proteins with an optimized length of the signal segment upstream of the prM–E domain [13]. Among the growing colonies under selection with 10 μg/mL of BS, the #22 colony cells released the highest levels of WNV antigens screened by ELISA and were cloned by two rounds of a limiting dilution method, resulting in the clones #22.6 and #22.6.6. These cloned cells stably secreted WNV antigens during long-term cell passages, whereas the expression levels of the parental #22 cells decreased and the antigens were undetectable at passage 31 (Fig. 1A).

The #22.6 clone was adapted to serum-free medium SFM-II by sequential subcultures in 25-cm^2 flasks with stepwise reduced FBS in growth medium. The adapted clone, designated #22.6S, was established at the 26th passage as suspension cells. The #22.6S cells continuously released WNV antigens during long-term passages in serum-free medium, although they produced less WNV antigens in subculture conditions than the parental #22.6 adherent cells (Fig. 1B).

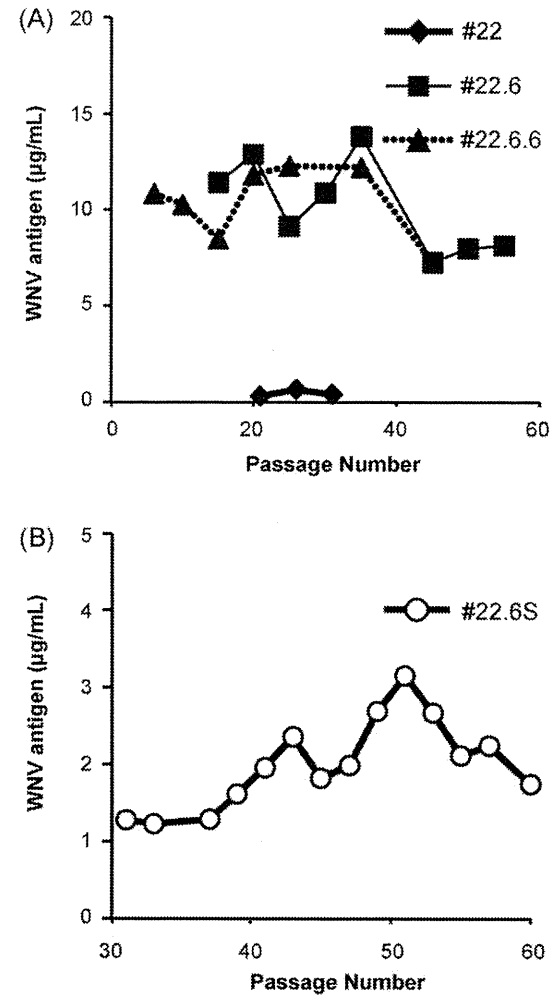

Fig. 1. Stable secretion of WNV prM–E antigen from established cell clones. The culture supernatants of (A) #22, #22.6 and #22.6.6 clone cells grown in F12K medium containing 10% FBS and (B) #22.6S cells cultured in serum-free medium SFM-II were collected at passages indicated and the amounts of secreted WNV antigens were measured by an antigen-capture ELISA. #22.6S cells cryopreserved at the 30th passage were recovered from a frozen stock.

3.2. Characterization of WNV antigens produced by the established clones

WNV antigens produced by the established clones were analyzed by immunoblotting with a JEV/WNV cross-reactive antiserum (the upper panels) and an anti-WNV M polyclonal antibody (the lower panels) (Fig. 2). The E and M proteins were detected as main bands, and the prM precursor protein was a minor band in the culture supernatants of both the adherent (#22.6 and #22.6.6) and suspending (#22.6S and #22.6.6S) cell clones (Fig. 2A). On the other hand, the cell lysates of the clones contained larger amounts of the prM protein than those of the M protein. This was also the case for WNV-infected Vero cells (Fig. 2B). These results indicate that the prM–E polyprotein produced in the established cell clones is successfully processed by host proteases during the transport through the cellular secretory pathway, regardless of adhesive and suspending properties of the cells. On the basis of these results, #22.6S cells were used in the following experiments.

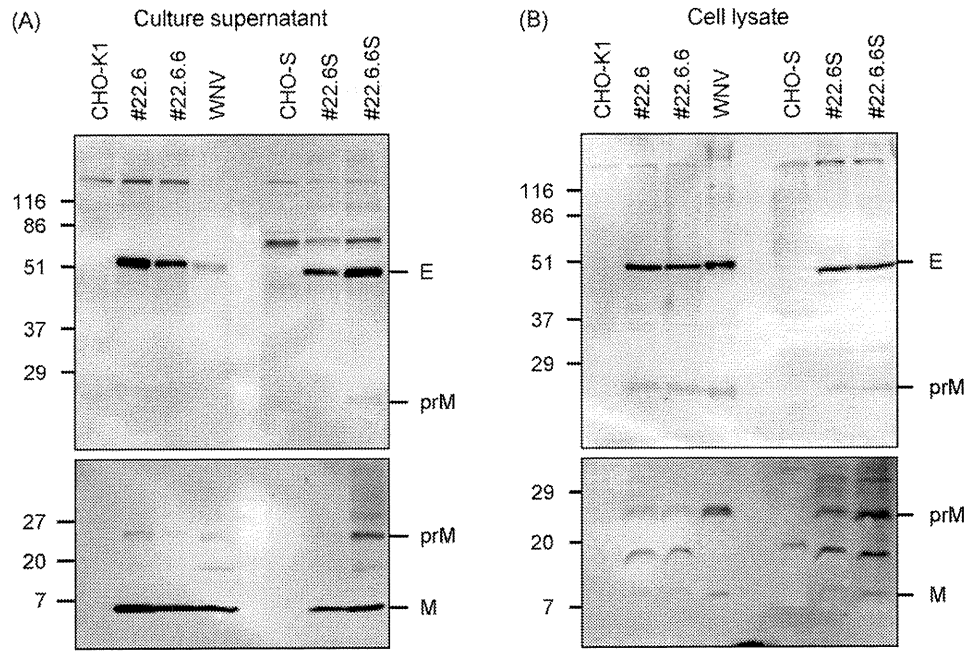

Fig. 2. Immunoblotting analyses of WNV antigens produced by cell clones. (A) Pellets from the culture supernatants and (B) the cell lysates were subjected to SDS-PAGE and analyzed with rabbit anti-JEV/WNV cross-reactive serum (upper panels) and rabbit anti-WNV M polyclonal antibody (lower panels). The positions of the E, prM and M proteins are indicated at the right. The molecular weights are shown in kilo-Daltons at the left.

Glycosylation status of the E and prM proteins expressed by #22.6S cells was analyzed with PNGase F that removes all N-linked glycans and with Endo H_f that removes only immature, high mannose-type glycans (Fig. 3). The E and prM proteins in the #22.6S culture supernatants were not affected by digestion with Endo H_f but decreased in their molecular masses by treatment with PNGase F. Similar results were obtained for WNV virions secreted from infected Vero cells, although the prM protein was not visible probably due to its low contents (Fig. 3A). Therefore, the E and prM proteins released from #22.6S cells appear to be in a mature glycosylation status similar to the virion proteins. In contrast to the culture supernatants, the E and prM proteins in lysates from #22.6S and WNV-infected cells were partially digested with Endo H_f, indicating that the E and prM proteins inside cells were dominantly in an immaturely glycosylated form (Fig. 3B). Consequently, these results suggest that #22.6S cells produce the E and prM proteins with immature sugar chains and release them in an Endo H-resistant mature form as WNV-infected cells do [9].

3.3. *Particle formation by prM–E expressing #22.6S cells*

WNV antigens secreted from #22.6S cells were observed by electron microscopy. Culture supernatants of #22.6S cells were concentrated by PEG precipitation and partially purified by Sephacryl S-300 chromatography to remove substrates smaller than 1.5 MDa. Fig. 4A shows large (40–50 nm) and small (20–30 nm) spherical particles together with irregular structures smaller than 5 nm. The small irregulars were also observed in culture supernatants of CHO-S cells that express no WNV antigens (Fig. 4B). These results show that #22.6S cells secrete WNV antigens in the forms of VLPs, which appeared, however, to be contaminated with the host cell-derived microsomal vesicles or debris.

In order to recover the spherical particles, the VLP preparation from #22.6S cultures was fractionated by equilibrium 10–50% sucrose density gradient centrifugation. WNV antigens were detected by ELISA as a single peak at the fraction of approximately 30% sucrose (density = 1.15 g/mL) (Fig. 4C). Unexpectedly,

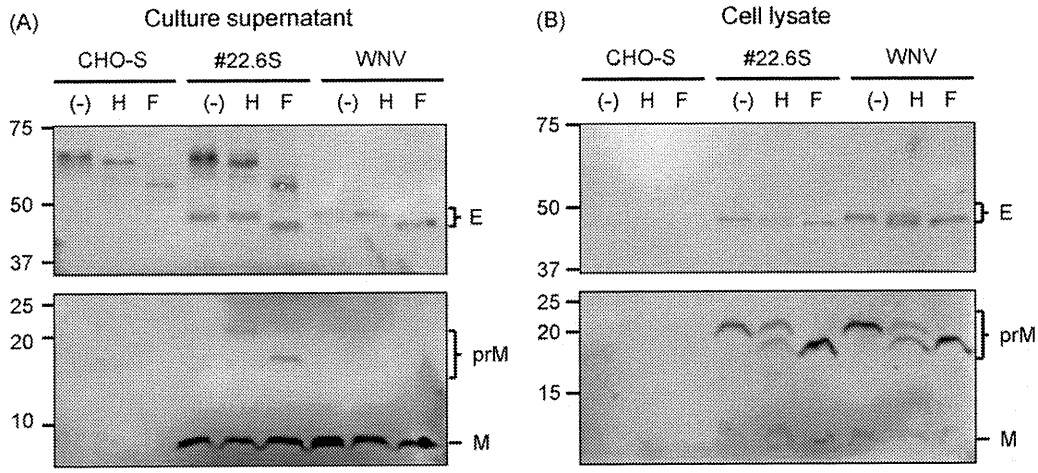

Fig. 3. Glycosylation status of WNV antigens produced by #22.6S cells. (A) Precipitates of the culture supernatants and (B) the cell lysates of CHO-S, #22.6S or WNV-infected Vero cells were digested with endoglycosidase Endo H_f (H) and PNGase F (F), or untreated (–). Digested proteins were examined by SDS-PAGE and immunoblotting.

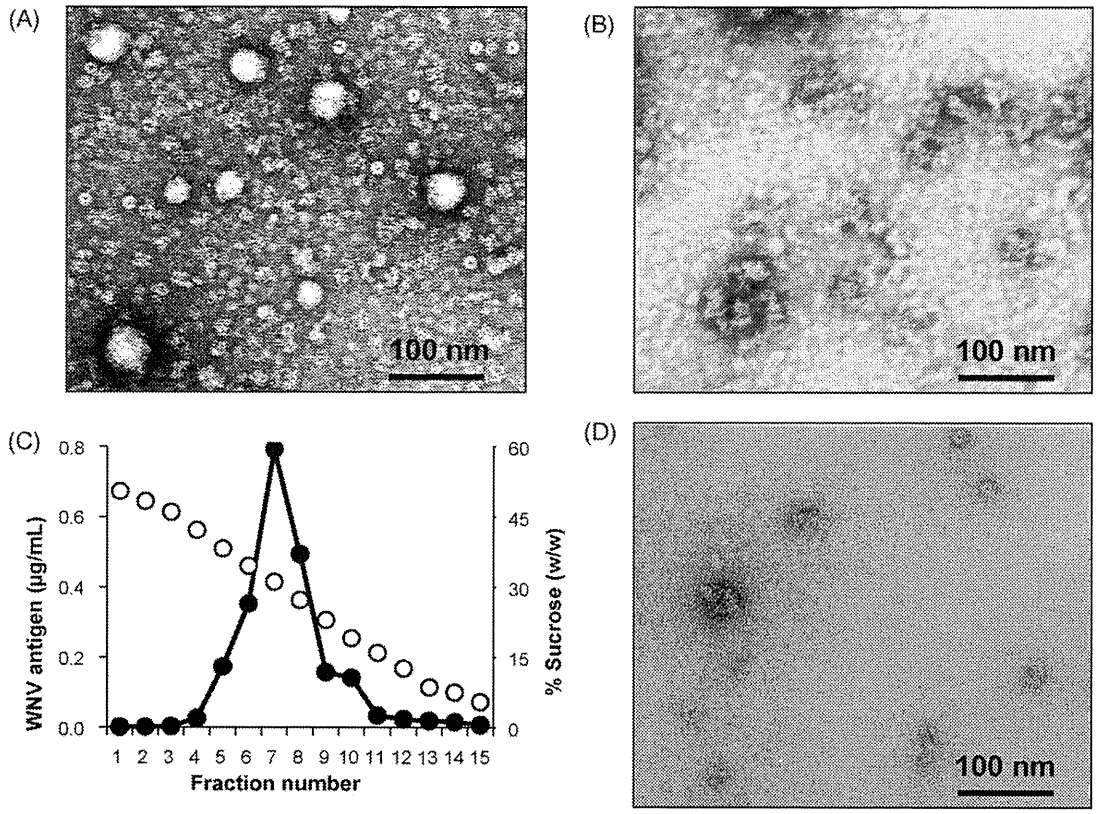

Fig. 4. Electron micrographs of WNV antigens released from #22.6S cells. The specimens prepared from the culture supernatants of (A) #22.6S clone cells and (B) CHO-S cells were observed after negative staining. (C) The culture supernatant of #22.6S cells was fractionated by equilibrium sedimentation on a 10–50% linear sucrose gradient at 160,000 × *g* for 15 h. Each fraction was examined for WNV antigens by ELISA (closed circles) and for sucrose concentrations (open circles). (D) The peak fraction in (C) was observed. Bars indicate 100 nm.

the peak fraction was abundant in severely shrunken structures and the spherical particles shown in Fig. 4A were scarcely observed by electron microscopy (Fig. 4D). The shrunken VLP antigens (named *Eq*-VLPs) were also observed abundantly when sucrose was added to the VLP preparations up to 30% (data not shown). From these results, we conclude that the spherical VLPs produced by #22.6S cells are vulnerable at sucrose concentrations over 30% and that equilibrium sucrose density gradient centrifugation is unsuitable for preparing intact VLPs.

3.4. Separation of VLPs by velocity sedimentation

Attempts were made to separate VLPs from small microstructures by velocity sedimentation in a gradient prepared with lower concentrations of sucrose. Culture supernatants of #22.6S cells were loaded to a linear 5–20% sucrose gradient and ultracentrifuged for 2 h. Fig. 5A clearly shows that WNV VLPs were separated into two peaks, that is in the fast sedimenting fraction at 18% sucrose (density = 1.07 g/mL) and in the slowly sedimenting fraction at 10% sucrose (density = 1.04 g/mL). These fast and slowly sedimenting VLPs were also recovered at the fractions of 19% and 14% sucrose, respectively, on a preparative scale by discontinuous 0%, 13% and 20% sucrose gradient centrifugation (Fig. 5B). The fast sedimenting VLPs were electron-dense, spherical and relatively large (40–50 nm in diameter) particles and slightly contaminated with small shrunken vesicles (Fig. 5C). On the other hand, smaller (20–30 nm) VLPs were abundantly observed in a slowly sedimenting zone, although irregular structures were also fractionated in the zone (Fig. 5D).

VLPs in the two peak fractions were collected by ultracentrifugation and examined by immunoblotting (Fig. 5E). Both VLP fractions contained the WNV E protein (the upper panel). The processed mature M protein of WNV was mainly detected in the fast sedimenting VLP fraction, whereas the unprocessed immature prM protein was a major component in the slowly sedimenting VLP fraction (the lower panel). Taken together, large, spherical and fully mature VLPs can be preparatively separated by velocity sedimentation from small, immature VLPs. These two VLPs with fast and slow velocities are distinctly termed *F*-VLPs and *S*-VLPs, respectively.

3.5. Antibody responses induced by VLPs with different particulate forms

Immunogenicity of *Eq*-VLPs, *F*-VLPs and *S*-VLPs was examined in mice experiments. Peak fractions collected by equilibrium or velocity sedimentation were cleared by Sephacryl S-300 chromatography. The VLP preparations were adjusted to the same OD value for the E antigen by ELISA as inactivated WNV that contains 1 μg/mL of protein, and were measured for protein amounts by the Lowry method. *Eq*-VLPs, *F*-VLPs and *S*-VLPs contained 20.7, 16.4 and 44.2 μg protein/mL, indicating that their purity is different and much low compared to inactivated WNV. Therefore, ELISA-normalized doses of the VLP antigens were used for immunization.

Groups of five mice were intraperitoneally injected twice with 100 ng (Table 1, Expt. 1) or 30–270 ng (Table 1, Expt. 2) of the VLP antigens and inactivated WNV as a positive control. NTAb titers in pooled sera from each group were determined by a $PRNT_{50}$ assay. *F*-VLPs induced higher NTAb titers in mice than *S*-VLPs (Expt. 1). In a dose–response experiment (Expt. 2), NTAb titers increased with immunizing doses of *F*-VLPs. In contrast, *S*-VLPs developed decreasing NTAb titers. The highest dose (270 ng) of *S*-VLPs was unable to improve the induction of NTAbs, and the titer was as low as 1: 40. Mice immunized with *Eq*-VLPs showed a rise of NTAb titers in doses from 30 to 90 ng but a decrease over 90 ng. NTAb titers induced with

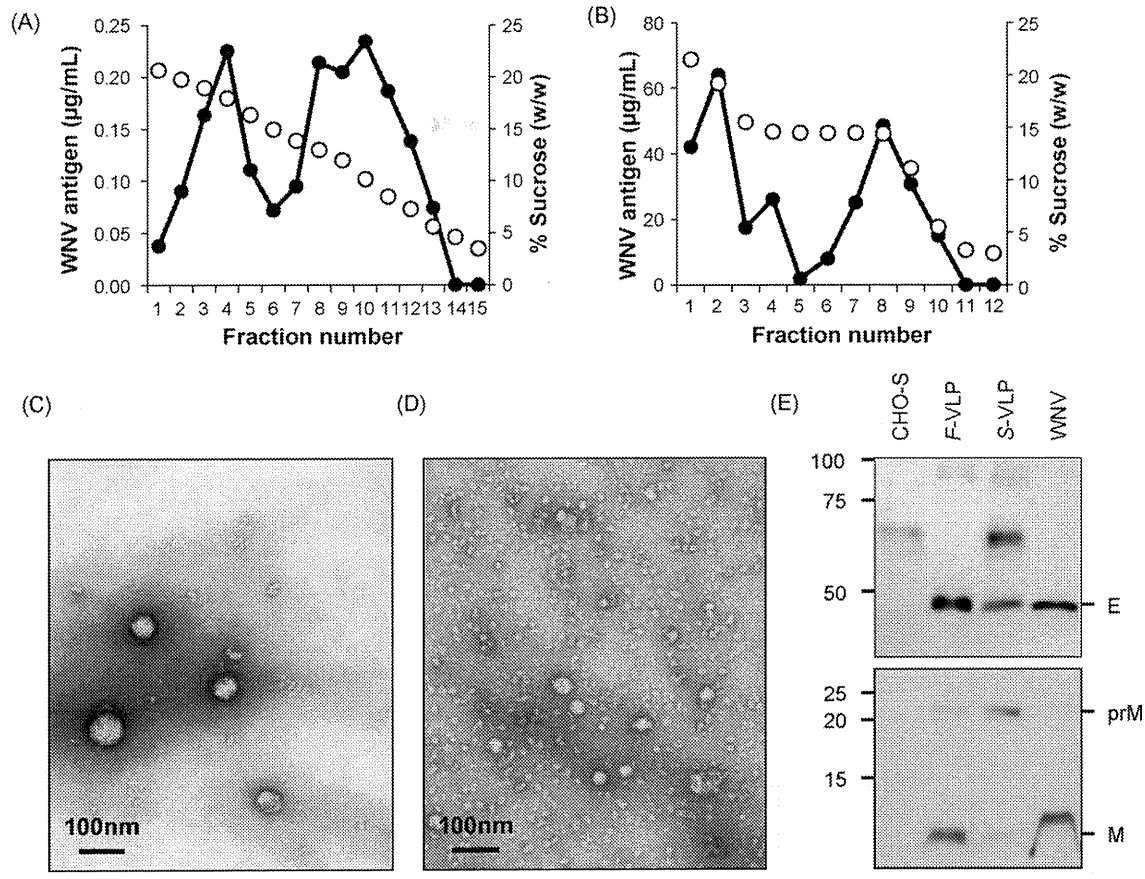

Fig. 5. Separation of released VLPs by velocity sedimentation. (A) The culture supernatant of #22.6S cells was subjected to 5–20% linear sucrose gradient centrifugation at 160,000 × *g* for 2 h. (B) For VLP preparation, the concentrated culture supernatants of #22.6S cells were centrifuged on a 0–13–20% discontinuous sucrose gradient. The sedimenting direction is right (top) to left (bottom). (C) The fast sedimenting (fraction 2) and (D) slowly sedimenting (fraction 8) antigens separated in (B) were observed by electron microscopy. (E) The fast and slowly sedimenting VLPs separated as in (B) were analyzed by immunoblotting with rabbit anti-JEV/WNV cross-reactive serum (upper panel) and rabbit anti-WNV M polyclonal antibody (lower panel).

formalin-inactivated WNV were higher than those with the VLP antigens, probably because it was highly purified and contained no impurities.

Antigen-specific IgG titers in mice immunized with 30–270 ng of VLPs were determined by ELISA using formalin-inactivated WNV as a coating antigen (Fig. 6). Total IgG to WNV increased in mice with immunizing antigen doses for *Eq*-VLPs and *F*-VLPs. However, immunization with 270 ng of *S*-VLPs induced no higher levels of anti-WNV IgG than that with 90 ng. Inactivated WNV elicited high levels of IgG in vaccinated mice (Fig. 6A). Antibody responses induced with the different forms of VLPs were further examined for ELISA titers of WNV-specific IgG1 and IgG2a isotypes. Mice infected with WNV or vaccinated with formalin-inactivated WNV developed low titers of IgG1 and considerably higher titers of IgG2a. This IgG2a-dominant antibody response was also observed in mice immunized with a high dose (270 ng) of morphologically intact *F*-VLPs (Fig. 6B). Even when lower doses (30 and 90 ng) of *F*-VLPs were used for immunization, IgG2a was dominant over IgG1 (data not shown). In mice immunized with *S*-VLPs, however, both IgG1 and IgG2a titers were low and substantially similar levels. In addition, *Eq*-VLPs induced no different levels of IgG1 and IgG2a antibodies (Fig. 6B).

These results indicate that among morphologically distinct VLPs, *F*-VLPs most closely resembling WNV particles in morphology are most similar to the wild-type whole virions in inducing antibody responses to the virus.

Table 1
Induction of neutralizing antibody titers in mice immunized with VLPs.

Immunizing antigen	Neutralizing antibody titer ($PRNT_{50}$)			
	Expt. 1	Expt. 2		
	100 ng	30 ng	90 ng	270 ng
F-VLPs	1:80	1:80	1:80	1:160
S-VLPs	1:20	1:80	1:80	1:40
Eq-VLPs	ND[a]	1:80	1:160	1:80
Inactivated WNV	1:160	1:640	1:1280	1:1280
PBS	<1:20		<1:20	

Groups of five 4-week-old C3H/HeN mice were immunized twice at 1-week interval with 100 ng (Expt. 1) or 30–270 ng (Expt. 2) of the VLP antigens and inactivated WNV. Sera were collected 1 week after the second immunization. NTAb titers of the pooled sera were examined by a plaque assay on Vero cell monolayers and expressed as the maximum serum dilution that resulted in a 50% reduction of plaque numbers ($PRNT_{50}$). *F*-VLPs and *S*-VLPs were recovered as the fast and slowly sedimenting fractions, respectively, from a discontinuous sucrose gradient. *Eq*-VLPs were the peak fraction by equilibrium sedimentation.

[a] ND: not done.

3.6. Protective efficacy of VLPs

Protective efficacy of the distinct types of VLPs was examined in a lethal mouse model of WNV infection. Six-week-old C3H/He mice were infected with 1, 10^1, 10^2 and 10^3 pfu of WNV. All the mice inoculated with 10^2 and 10^3 pfu of WNV were developed severe clinical signs and died within 10 days, whereas 10 pfu of the virus did not cause 100% lethality and a challenge dose of 1 pfu showed no virulence in mice for 14 days (Fig. 7A). Thus, 10^3 pfu of WNV were used for lethal infection. Mice were vaccinated twice with 90 ng of

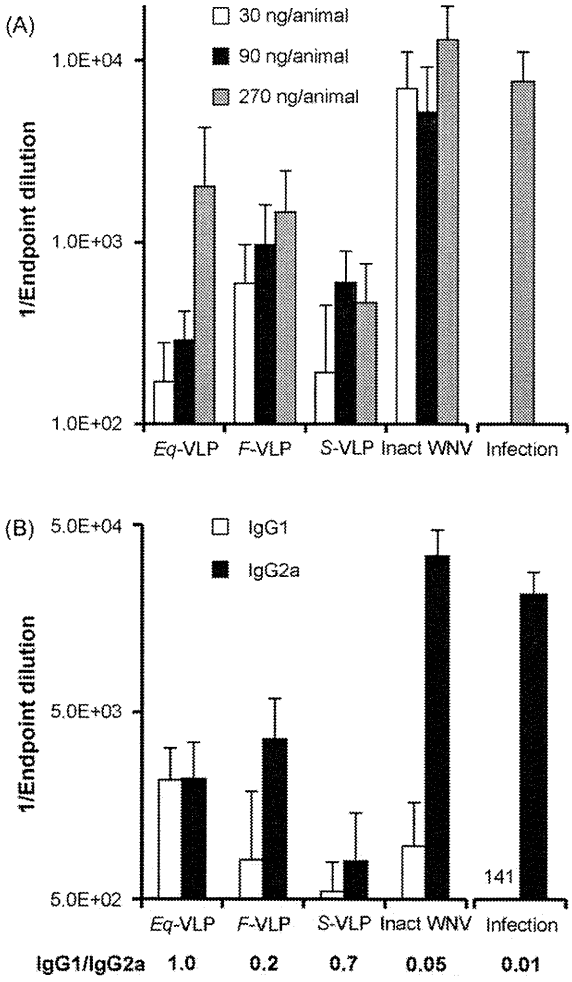

Fig. 6. WNV-specific IgG ELISA endpoint titers in mice immunized with VLPs. (A) Mice were immunized as in Table 1 and total IgG antibody titers in sera were determined by ELISA on plates coated with formalin-inactivated WNV. IgG titers in mice survived WNV infection were also shown. The cutoff values were calculated from the O.D. values of the PBS (−)-injected mouse sera. The results show the means and standard deviations. (B) Titers of IgG1 and IgG2a subclasses in mice immunized with 270 ng of VLPs were determined as in (A).

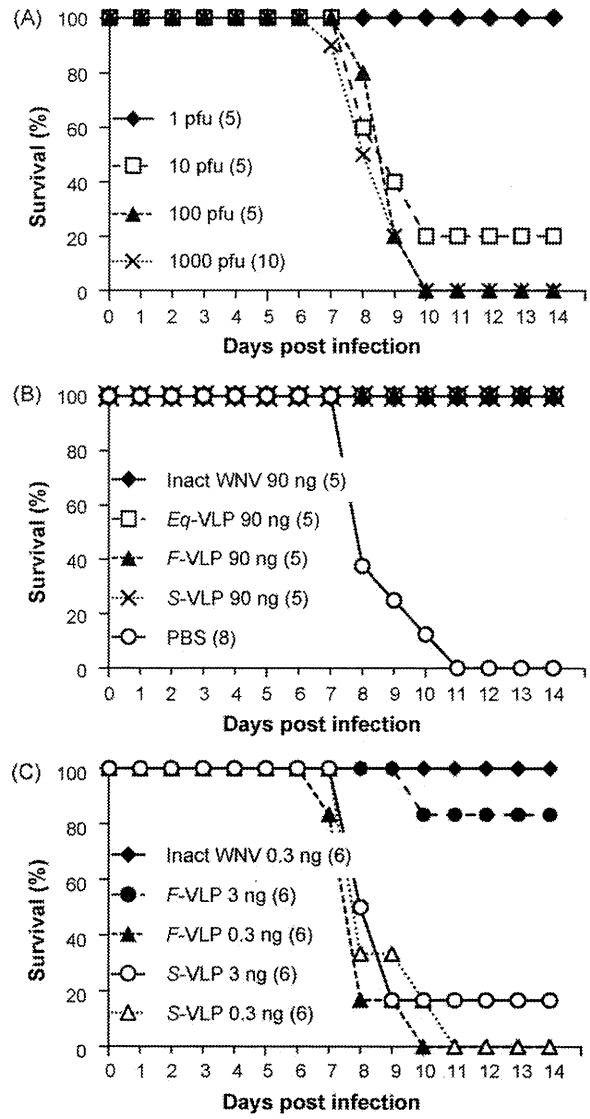

Fig. 7. Protective efficacy of VLPs against lethal WNV challenge. (A) Naïve C3H/HeN mice (6-week old) were intraperitoneally infected with 1, 10^1, 10^2 and 10^3 pfu of the WNV NY-99 strain and observed for 14 days. (B) Groups of C3H/HeN mice (4-week old) were vaccinated twice with a high dose (90 ng) of VLPs and intraperitoneally challenged with 10^3 pfu of WNV at 1 week post-vaccination. (C) Mice were vaccinated with low doses (3 and 0.3 ng) of VLPs and challenged with WNV as in (B). The number of mice in each group is shown in the parentheses of each graph.

the three types of VLPs as in immunization experiments and were challenged at the age of 6 weeks with 10^3 pfu of WNV. Fig. 7B shows that a high dose (90 ng) of the VLP antigens rendered mice protective against WNV and mice vaccinated with *Eq*-VLPs, *F*-VLPs and *S*-VLPs survived 100% without detectable clinical signs. In order to examine whether *F*-VLPs and *S*-VLPs are different in their ability to develop protective immunity, low doses (3 and 0.3 ng) of *F*-VLPs and *S*-VLPs were inoculated into groups of six mice. These mice were challenged with 10^3 pfu of WNV and observed daily for 2 weeks (Fig. 7C). Five out of six (83%) mice immunized with 3 ng of *F*-VLPs were survived from the lethal dose of WNV infection. In contrast to *F*-VLPs, the same dose of *S*-VLPs saved only one (17%) mouse. Mice receiving a much lower dose (0.3 ng) of *F*-VLPs and *S*-VLPs similarly showed the clinical course of infection and died 100%, although all the mice survived with 0.3 ng of inactivated WNV. These results suggest that *F*-VLPs are superior to *S*-VLPs in immunogenicity and protective efficacy against WNV as well.

4. Discussion

We have successfully established CHO #22.6S cells that continuously express the WNV prM–E gene and stably produce WNV VLPs in serum-free cultures. In this study, two distinct types of VLPs were found to be secreted from the established cells; larger (40–50 nm in diameter) *F*-VLPs and smaller (20–30 nm in diameter) *S*-VLPs, which could be separated by velocity sedimentation. So far, two distinct size classes of flaviviral VLPs were only observed by the expression of the tick-borne encephalitis virus (TBEV) prM–E gene in transfected COS-1 cells [33]. Previous studies on the flavivirus morphogenesis argued that packaging of the viral RNA into a core composed of the C proteins was a prerequisite to form particles in the virion sizes [34]. However, our *F*-VLPs of WNV and their large RSPs of TBEV are similar in size to the original whole viruses without the C proteins. Both large VLPs and RSPs were distinguished from small ones by velocity sedimentation in gradients prepared with lower concentrations of sucrose, and were fractionated at similar migration rates. The mature M proteins were a major component of the large VLP/RSP particles, when generated from the wild-type prM–E genes of WNV and TBEV. However, RSPs with the immature prM protein were produced in a large size from a TBEV prM–E gene derivative by a mutation at the furin cleavage site. On the other

hand, *S*-VLPs and small RSPs have similar appearances to prM/M–E VLPs of other flaviviruses [10–12]. It is known that flavivirus-infected cells produce not only infectious virus particles but smaller noninfectious particles called slowly sedimenting hemagglutinin (SHA). SHAs are separated from the virions by sucrose gradient centrifugation and show similar sedimenting profiles to prM/M–E VLPs [15,35]. Taken together, *F*-VLPs and *S*-VLPs may be analogous to infectious virions and SHAs, respectively.

Interestingly, the processed mature M and unprocessed immature prM proteins were major and minor, respectively, in larger *F*-VLPs; reversely in smaller *S*-VLPs, however, the M and prM proteins were minor and major, respectively (Fig. 5E). This result may suggest some effects of proteolytic processing of prM into M on VLP sizes. The prM and E proteins of flaviviruses are thought to associate into heterodimers, to assemble into immature particles and to bud into the lumen of the ER in small SHA or VLP size. During traffic through the secretory pathway, a significant portion of prM is cleaved by host furin protease in the trans-Golgi to form the M protein. Recent X-ray crystallography of the E proteins and cryo-electron microscopy of the flavivirus particles have proposed a model where trimeric prM/E heterodimers form progenitor particles and processing of prM into M allows to generate E homodimers in association with mature M and to form infectious viruses with diameters of about 50 nm [7,8]. Similarly to the model, the prM cleavage of smaller VLPs in the Golgi might induce the conformational rearrangement of the prM/E heterodimers to the E homodimers associated with processed M and make the small particles appear larger, although prM-unprocessed particles preserve small VLP size. In addition, several papers suggest the processing effects. The disruption of cellular furin protease or the improper digestion by host signalase decreases viral infectivity and increases the production of small, noninfectious SHAs [36,37]. The proportion of the immature prM proteins to total prM/M proteins is high in SHAs and that of the mature M proteins is high in the whole virions [35].

Glycosylation of the structural proteins is a constitutive factor that affects flavivirus assembly [9]. Thus, the ratios of large and small VLPs are possibly regulated by the modification with sugar chains. The sizes of our VLPs are, however, unlikely to depend on the glycosylation status, since the E proteins of WNV VLPs were resistant to Endo H_f digestion as WNV virions. In case of TBEV RSPs, on the other hand, the E glycoproteins of the larger particles were slightly more sensitive to Endo H_f glycosidase than those of the smaller particles [33]. Although subtle differences in the structural environment of the sugar chains are discussed for TBEV RSPs, subtle delays in the processing of the prM–E polyprotein may happen to our *F*- and *S*-VLPs in intracellular transport pathways and alter the relative release rate of large and small VLPs.

If the processed M and unprocessed prM proteins could differentially modulate the organization of the E proteins on large and small VLPs, it is possible that *F*- and *S*-VLPs are different in their antigenic forms. Thus, it is important to address antibody responses induced with *F*-VLPs and *S*-VLPs. Our results show that *F*-VLPs were superior to other forms of VLPs. NTAb titers against WNV increased with immunizing doses of *F*-VLPs. However, small *S*-VLPs and shrunken *Eq*-VLPs induced lower levels of NTAbs at higher immunizing doses. Furthermore, IgG2a-dominant antibody responses were induced by *F*-VLPs and the whole virion-derived antigens, such as formalin-inactivated and infectious viruses, but not by *S*-VLPs and *Eq*-VLPs. These data are consistent with the previous studies revealing that the recombinant TBEV antigens forming subviral particles and the attenuated replicons could induce high NTAb titers with IgG2a dominance [38–40]. Therefore, the E proteins of *F*-VLPs appear to be rearranged upon prM cleavage to more immunogenic conformations.

In contrast to *F*-VLPs, *S*-VLPs were a poorer immunogen. Levels of IgG antibodies were low and not dominant to the IgG2a subclass. NTAb titers unexpectedly decreased with increasing *S*-VLP dose. The *S*-VLP preparation contained a considerable amount of CHO-S-derived cellular debris. Therefore, a possibility is that the contaminating cellular proteins from CHO lines expressing prM–E may be cross-reactive and inhibit immunogenic stimulus on B-cell clones at high doses of the *S*-VLP preparation. However, the shrunken *Eq*-VLP preparation in which the cellular microsomal vesicles or debris were rather a low amount, induced antibody responses as the *S*-VLP preparation did in terms of NTAb titers and the IgG subclass distribution. Furthermore, *S*-VLPs were observed as clearly distinct particles from *F*-VLPs in both size and appearance. Therefore, differences in the morphological forms between *F*-VLPs and *S*-VLPs are likely to reflect their immunogenicity to induce protective antibody responses.

All types of our VLPs, however, completely protected mice against WNV infection when a sufficient dose (90 ng per animal) was used for immunization. The critical roles of antibodies have been described to protect against WNV-induced mortality [17,18] and the high dose (90 ng) of VLPs all induced substantial levels of NTAb titers. In contrast, a low dose (3 ng) of *F*-VLPs showed apparently higher protective efficacy against WNV than *S*-VLPs. In addition to NTAbs, *F*-VLPs possessed antigenicity favorable to IgG2a-dominant antibody responses, which are promoted by T-helper 1 lymphocytes that are responsible for inducing cell-mediated immune responses [38,39,41]. Besides NTAbs, cytotoxic T-lymphocyte responses are also known to have an important function in flavivirus clearance [42]. Thus, the different morphological forms of VLPs appear to affect the host defense against WNV pathogenesis and large *F*-VLPs are able to induce better protective immunity than small *S*-VLPs.

In summary, we have succeeded in separating immunogenic *F*-VLPs from *S*-VLPs and host cell-derived impurities, and suggested that large *F*-VLPs produced in serum-free cultures of #22.6S cell clones are a promising candidate as a second-generation WNV vaccine. To accomplish it, the optimization of sucrose density gradient centrifugation was needed for purification of the large, mature *F*-VLPs without shrinkage of the particles. The procedures described here would be applicable for other flavivirus VLPs as well as the viral replicon particles and attenuated virions [20–23] to refining their immunogenicity as flavivirus vaccines.

Acknowledgements

This work was supported in part by research grants from the Ministry of Health, Labor, and Welfare, and from the Japanese Health Sciences Foundation (A. Kojima).

References

[1] Dauphin G, Zientara S. West Nile virus: recent trends in diagnosis and vaccine development. Vaccine 2007;25(July (30)):5563–76.
[2] Iwamoto M, Jernigan DB, Guasch A, Trepka MJ, Blackmore CG, Hellinger WC, et al. Transmission of West Nile virus from an organ donor to four transplant recipients. N Engl J Med 2003;348(May (22)):2196–203.
[3] Pealer LN, Marfin AA, Petersen LR, Lanciotti RS, Page PL, Stramer SL, et al. Transmission of West Nile virus through blood transfusion in the United States in 2002. N Engl J Med 2003;349(September (13)):1236–45.
[4] Kuhn RJ, Zhang W, Rossmann MG, Pletnev SV, Corver J, Lenches E, et al. Structure of dengue virus: implications for flavivirus organization, maturation, and fusion. Cell 2002;108(March (5)):717–25.
[5] Mukhopadhyay S, Kim BS, Chipman PR, Rossmann MG, Kuhn RJ. Structure of West Nile virus. Science 2003;302(October (5643)):248.
[6] Lorenz IC, Allison SL, Heinz FX, Helenius A. Folding and dimerization of tick-borne encephalitis virus envelope proteins prM and E in the endoplasmic reticulum. J Virol 2002;76(June (11)):5480–91.
[7] Li L, Lok SM, Yu IM, Zhang Y, Kuhn RJ, Chen J, et al. The flavivirus precursor membrane-envelope protein complex: structure and maturation. Science 2008;319(March (5871)):1830–4.

[8] Zhang Y, Kaufmann B, Chipman PR, Kuhn RJ, Rossmann MG. Structure of immature West Nile virus. J Virol 2007;81(June (11)):6141–5.
[9] Hanna SL, Pierson TC, Sanchez MD, Ahmed AA, Murtadha MM, Doms RW. N-linked glycosylation of west nile virus envelope proteins influences particle assembly and infectivity. J Virol 2005;79(November (21)):13262–74.
[10] Konishi E, Pincus S, Paoletti E, Shope RE, Burrage T, Mason PW. Mice immunized with a subviral particle containing the Japanese encephalitis virus prM/M and E proteins are protected from lethal JEV infection. Virology 1992;188(June (2)):714–20.
[11] Mutoh E, Ishikawa T, Takamizawa A, Kurata T, Sata T, Kojima A. Japanese encephalitis subunit vaccine composed of virus-like envelope antigen particles purified from serum-free medium of a high-producer J12#26 cell clone. Vaccine 2004;22(June (20)):2599–608.
[12] Schalich J, Allison SL, Stiasny K, Mandl CW, Kunz C, Heinz FX. Recombinant subviral particles from tick-borne encephalitis virus are fusogenic and provide a model system for studying flavivirus envelope glycoprotein functions. J Virol 1996;70(July (7)):4549–57.
[13] Takahashi H, Ohtaki N, Maeda-Sato M, Tanaka M, Tanaka K, Sawa H, et al. Effects of the number of amino acid residues in the signal segment upstream or downstream of the NS2B-3 cleavage site on production and secretion of prM/M–E virus-like particles of West Nile virus. Microbes Infect 2009;11(November (13)):1019–28.
[14] Ferlenghi I, Clarke M, Ruttan T, Allison SL, Schalich J, Heinz FX, et al. Molecular organization of a recombinant subviral particle from tick-borne encephalitis virus. Mol Cell 2001;7(March (3)):593–602.
[15] Mason PW, Pincus S, Fournier MJ, Mason TL, Shope RE, Paoletti E. Japanese encephalitis virus-vaccinia recombinants produce particulate forms of the structural membrane proteins and induce high levels of protection against lethal JEV infection. Virology 1991;180(January (1)):294–305.
[16] Chiba N, Osada M, Komoro K, Mizutani T, Kariwa H, Takashima I. Protection against tick-borne encephalitis virus isolated in Japan by active and passive immunization. Vaccine 1999;17(March (11–12)):1532–9.
[17] Diamond MS, Shrestha B, Marri A, Mahan D, Engle M. B cells and antibody play critical roles in the immediate defense of disseminated infection by West Nile encephalitis virus. J Virol 2003;77(February (4)):2578–86.
[18] Engle MJ, Diamond MS. Antibody prophylaxis and therapy against West Nile virus infection in wild-type and immunodeficient mice. J Virol 2003;77(December (24)):12941–9.
[19] Oya A. Japanese encephalitis vaccine. Acta Paediatr Jpn 1988;30(April (2)):175–84.
[20] Widman DG, Ishikawa T, Fayzulin R, Bourne N, Mason PW. Construction and characterization of a second-generation pseudoinfectious West Nile virus vaccine propagated using a new cultivation system. Vaccine 2008;26(May (22)):2762–71.
[21] Yu L, Robert Putnak J, Pletnev AG, Markoff L. Attenuated West Nile viruses bearing 3'SL and envelope gene substitution mutations. Vaccine 2008;26(November (47)):5981–8.
[22] Monath TP, Liu J, Kanesa-Thasan N, Myers GA, Nichols R, Deary A, et al. A live, attenuated recombinant West Nile virus vaccine. Proc Natl Acad Sci U S A 2006;103(April (17)):6694–9.
[23] Pletnev AG, Swayne DE, Speicher J, Rumyantsev AA, Murphy BR. Chimeric West Nile/dengue virus vaccine candidate: preclinical evaluation in mice, geese and monkeys for safety and immunogenicity. Vaccine 2006;24(September (40–41)):6392–404.
[24] Despres P, Combredet C, Frenkiel MP, Lorin C, Brahic M, Tangy F. Live measles vaccine expressing the secreted form of the West Nile virus envelope glycoprotein protects against West Nile virus encephalitis. J Infect Dis 2005;191(January (2)):207–14.
[25] Martin JE, Pierson TC, Hubka S, Rucker S, Gordon IJ, Enama ME, et al. A West Nile virus DNA vaccine induces neutralizing antibody in healthy adults during a phase 1 clinical trial. J Infect Dis 2007;196(December (12)):1732–40.
[26] Lim CK, Takasaki T, Kotaki A, Kurane I. Vero cell-derived inactivated West Nile (WN) vaccine induces protective immunity against lethal WN virus infection in mice and shows a facilitated neutralizing antibody response in mice previously immunized with Japanese encephalitis vaccine. Virology 2008;374(April (1)):60–70.
[27] Bonafe N, Rininger JA, Chubet RG, Foellmer HG, Fader S, Anderson JF, et al. A recombinant West Nile virus envelope protein vaccine candidate produced in *Spodoptera frugiperda* expresSF+ cells. Vaccine 2009;27(January (2)):213–22.
[28] Lieberman MM, Clements DE, Ogata S, Wang G, Corpuz G, Wong T, et al. Preparation and immunogenic properties of a recombinant West Nile subunit vaccine. Vaccine 2007;25(January (3)):414–23.
[29] Martina BE, Koraka P, van den Doel P, van Amerongen G, Rimmelzwaan GF, Osterhaus AD. Immunization with West Nile virus envelope domain III protects mice against lethal infection with homologous and heterologous virus. Vaccine 2008;26(January (2)):153–7.
[30] Gehrke R, Ecker M, Aberle SW, Allison SL, Heinz FX, Mandl CW. Incorporation of tick-borne encephalitis virus replicons into virus-like particles by a packaging cell line. J Virol 2003;77(August (16)):8924–33.
[31] Konishi E, Fujii A, Mason PW. Generation and characterization of a mammalian cell line continuously expressing Japanese encephalitis virus subviral particles. J Virol 2001;75(March (5)):2204–12.
[32] Kojima A, Yasuda A, Asanuma H, Ishikawa T, Takamizawa A, Yasui K, et al. Stable high-producer cell clone expressing virus-like particles of the Japanese encephalitis virus e protein for a second-generation subunit vaccine. J Virol 2003;77(August (16)):8745–55.
[33] Allison SL, Tao YJ, O'Riordain G, Mandl CW, Harrison SC, Heinz FX. Two distinct size classes of immature and mature subviral particles from tick-borne encephalitis virus. J Virol 2003;77(November (21)):11357–66.
[34] Patkar CG, Jones CT, Chang YH, Warrier R, Kuhn RJ. Functional requirements of the yellow fever virus capsid protein. J Virol 2007;81(June (12)):6471–81.
[35] Ishikawa T, Konishi E. Mosquito cells infected with Japanese encephalitis virus release slowly-sedimenting hemagglutinin particles in association with intracellular formation of smooth membrane structures. Microbiol Immunol 2006;50(3):211–23.
[36] Junjhon J, Lausumpao M, Supasa S, Noisakran S, Songjaeng A, Saraithong P, et al. Differential modulation of prM cleavage, extracellular particle distribution, and virus infectivity by conserved residues at nonfurin consensus positions of the dengue virus pr-M junction. J Virol 2008;82(November (21)):10776–91.
[37] Lobigs M, Lee E. Inefficient signalase cleavage promotes efficient nucleocapsid incorporation into budding flavivirus membranes. J Virol 2004;78(January (1)):178–86.
[38] Aberle JH, Aberle SW, Allison SL, Stiasny K, Ecker M, Mandl CW, et al. A DNA immunization model study with constructs expressing the tick-borne encephalitis virus envelope protein E in different physical forms. J Immunol 1999;163(December (12)):6756–61.
[39] Aberle JH, Aberle SW, Kofler RM, Mandl CW. Humoral and cellular immune response to RNA immunization with flavivirus replicons derived from tick-borne encephalitis virus. J Virol 2005;79(December (24)):15107–13.
[40] Heinz FX, Allison SL, Stiasny K, Schalich J, Holzmann H, Mandl CW, et al. Recombinant and virion-derived soluble and particulate immunogens for vaccination against tick-borne encephalitis. Vaccine 1995;13(December (17)):1636–42.
[41] Finkelman FD, Holmes J, Katona IM, Urban Jr JF, Beckmann MP, Park LS, et al. Lymphokine control of in vivo immunoglobulin isotype selection. Annu Rev Immunol 1990;8:303–33.
[42] Shrestha B, Diamond MS. Role of CD8+ T cells in control of West Nile virus infection. J Virol 2004;78(August (15)):8312–21.

Induction of extremely low protein expression level by fusion of *C*-terminal region of Nef

Nobutoki Takamune[*1], Yukari Irisaka[*], Minami Yamamoto[*], Keisuke Harada[*], Shozo Shoji[*0], and Shogo Misumi[*]

[*]Department of Pharmaceutical Biochemistry, Faculty of Life Sciences, Kumamoto University, 5-1 Oe-Honmachi, Kumamoto 862-0973, Japan. [0]Kumamoto Health Science University, Kumamoto, 325 Izumimachi, Kumamoto 861-5598, Japan.

Running title : Induction of extremely low protein expression level

Address correspondence to: Nobutoki Takamune, PhD, 5-1 Oe-Honmachi, Kumamoto 862-0973, Japan.
Phone: +81-96-371-4367
Fax: +81-96-362-7800
E-mail: tkmnnbtk@gpo.kumamoto-u.ac.jp

Synopsis

Nef is one of the accessory proteins of human immunodeficiency viruses. Here, we noted that the relative expression level of Nef_{NL4-3} is much lower than that of Nef_{JR-CSF} in HEK293 cells. By evaluating the expression level using a Nef mutant, it was indicated that amino acids 129-206 of Nef_{NL4-3}, i.e., the *C*-terminal region named NLAA129-206, could contain the region responsible for the induction of the low protein expression level. Additionally, the expression levels of the enhanced green fluorescent protein (EGFP) and *Renilla* luciferase (Rluc) became extremely low with the fusion of NLAA129-206, Interestingly, the NLAA129-206-corresponding sequences of other Nef variants with relatively high expression levels also induced the extremely low protein expression level by fusion. These results suggest that the *C*-terminal region of Nef can generally induce an extremely low protein expression level. Here, we propose that the *C*-terminal region of Nef could become an excellent tool for the induction of an extremely low expression level of arbitrary proteins by attachment as fusion proteins.

Footnotes

Key words: enhanced green fluorescent protein (EGFP), human immunodeficiency virus (HIV), Nef, protein degradation sequence, *Renilla* luciferase (Rluc).

Abbreviations used: HIV, human immunodeficiency virus; SIV, simian immunodeficiency virus; HEK293, human embryonic kidney 293; EGFP, enhanced green fluorescent protein; Rluc, *Renilla* luciferase; DAPI, 4',6-diamidino-2-phenylindole dihydrochloride; SDS-PAGE, sodium dodecyl sulfate-polyacrylamide gel electrophoresis; UPS, ubiquitin proteasome system

[1]To whom correspondence should be address (email: tkmnnbtk@gpo.kumamoto-u.ac.jp)

Introduction

Nef, a 27-35-kDa protein, is one of the accessory proteins of human and simian immunodeficiency viruses (HIV and SIV, respectively) that enhance viral replication and is associated with the pathogenicity of these viruses. It has many functional motifs for contact to host proteins [1], by which it can serve as a molecular adaptor and exert multiple functions like CD4 downregulation and MHC class I downregulation [2]. Moreover, Nef can enhance viral infectivity, although the mechanism underlying such enhancement remains unclear [3]. *N*-myristoylation occurs at the *N*-terminus of Nef [4], and the posttranslational modification is essential for multiple functions [2].

Genetic diversity is one of the major characteristics of HIV and SIV [5]. We can find highly frequent mutations of amino acid substitution, insertion, and deletion among viral strains in the Los Alamos HIV database (http://hiv-web.lanl.gov). Such a genetic diversity can generate many viral phenotypes, resulting in, for example, CCR5 or CXCR4 usage [6], escape from the immune attack of the host [7], and the emergence of drug-resistant viruses [7].

The abundance of each protein is closely associated with the efficacy of its function, because protein activity is basically exerted in a dose-dependent manner. Protein expression level depends not only on mRNA level but also on translation rate and degradation rate [8, 9]. Protein degradation comprises two major systems: ubiquitin-mediated proteolysis and lysosomal degradation [10].

Some degradation signals conferring instability on proteins have been found, which include N-degrons [11], a murine ornithine decarboxylase (MODC) PEST region [12], and CL peptides [13]. These signals induce a rapid protein degradation mediated by a proteasome, in which the N-degron and CL peptides require ubiquitination

prior to degradation, while the PEST sequence is independent of ubiqutination [14]. The PEST sequence and CL peptides could convert stable proteins into unstable proteins by attachment as fusion proteins [13, 15,16], of which the apparent expression levels could be much lower than those of the original proteins [15-17]. The feature of the instability induction of the PEST sequence and CL peptides has been applied to the development of a highly responsive reporter system [18-20] and to the improvement of the recombinant protein productivity of CHO cells [21]. In addition to protein degradation signals, mRNA-destabilizing elements [22-24] are utilized for such a system [18].

Here, we clarified that the *C*-terminal region (amino acids 129-206) of Nef_{NL4-3} with an extremely low expression level is necessary and sufficient for the induction of the low expression level of reporter proteins by attachment as fusion proteins. Additionally, it was indicated that the *C*-terminal regions of not only Nef_{NL4-3} but also other Nef variants, which even show relatively higher expression levels, have an ability to induce low protein expression levels by attachment. The mechanism of this induction has not been fully resolved yet. We propose that the *C*-terminal region of Nef is applicable to the development of a highly responsive reporter system and to the improvement of recombinant protein productivity.

Materials and Methods

Nef expression vectors

DNAs coding Nef proteins were amplified by PCR using the corresponding proviral DNA template and subcloned into pcDNA^{TM}3.1D/V5-His TOPO according to the manufacturer's instructions (Invitrogen, Carlsbad, CA).

DNA coding Nef_{JR-CSF}-V5 or Nef_{NL4-3}-V5 was amplified by PCR using pcDNA3.1/Nef_{JR-CSF}-V5 and pcDNA3.1/Nef_{NL4-3}-V5, respectively, and subcloned into the pcDNA4/HisMax vector (Invitrogen, Carlsbad, CA) without polyhistidine and the Xpress^{TM} epitope-coding region. The expression vector for the Nef chimera was generated by standard overlapping PCR techniques [25].

The expression vector for each Nef Gly 2-to-Ala 2 (G2A) mutant was constructed by site-directed mutagenesis, as previously described [26].

Expression vectors of enhanced green fluorescent protein (EGFP) or *Renilla* luciferase (Rluc) fusion protein

Each expression vector for EGFP appended with each amino acid sequence to the *N*-terminal end was constructed using pEGFP-N1 (Clontech, Mountain View, CA), in which a triple repeat of the linker Gly-Gly-Gly-Gly-Ser [$(GGGGS)_3$] [27] and Xpress-epitope-tag-coding DNAs were respectively inserted at the *Sal*I-*Apa*I and *Hin*dIII-*Pst*I sites. Each expression vector for Rluc was constructed by replacing the EGFP-coding DNA with the Rluc-coding DNA of the multiple cloning site (MCS) of each EGFP expression vector. Each expression vector for EGFP appended with each amino acid sequence to the *C*-terminal end was constructed using a pcDNA4/HisMax vector, in which EGFP, the $(GGGGS)_3$ linker, and DNAs coding each amino acid sequence were respectively inserted in the *Kpn*I-*Bam*HI, *Bam*HI-*Eco*RI, and *Eco*RI-*Pst* I sites of the MCS of the vector.

Cell culture and transfection

Human embryonic kidney 293 (HEK293) cells were cultured and transfected using Lipofectamine LTX reagent, as previously described [26].

HEK293/CD4/Nef_{JR-CSF}, HEK293/CD4/Nef_{NL4-3}, HEK293/CD4/Nef_{JR-CSF} G2A, and HEK293/CD4/Nef_{NL4-3} G2A cells

HEK293/CD4 cells were transfected with the pcDNA4/HisMax vector for Nef_{JR-CSF}, Nef_{NL4-3}, Nef_{JR-CSF} G2A, and Nef_{NL4-3} G2A. 2 days after transfection, stable clones were selected in the presence of 500 μg/ml zeocin in the conditioned medium. Each clonal HEK293/CD4/Nef cell line was obtained by the limiting-dilution method.

Immunostaining analysis

The cells were rinsed and fixed with 1% fresh paraformaldehyde in PBS(-). After permeabilization with methanol, Nef was visualized using an anti-V5 antibody, followed by an anti-mouse-FITC secondary antibody. The nucleus was stained with 4',6-diamidino-2-phenylindole dihydrochloride (DAPI). The cells were observed using a Biozero digital microscope (Keyence, Osaka, Japan).

Cell lysis and western blot analysis

The cells were lysed in lysis buffer (50 mM Tris-HCl pH 8.0, 150 mM NaCl, 1% Triton X-100, protease inhibitors [1 mM 4-amidinophenylmethanesulfonyl fluoride hydrochloride (APMSF), 50 μg/ml aprotinin, 50 μg/ml leupeptin, 50 μg/ml pepstatin A, 50 μg/ml antipine]) and subjected to 5-20% polyacrylamide gradient sodium dodecyl sulfate-polyacrylamide gel electrophoresis (SDS-PAGE). Then, separated proteins on the gel were transferred to the polyvinylidene fluoride (PVDF) membrane. The membranes blocked by 5% skim-milk were incubated with an anti-V5 antibody or anti-Xpress antibody (Invitrogen, Carlsbad, CA) diluted 1:5000 in immunoenhancer reagent A (Wako, Osaka, Japan) for 4 h, and then with peroxidase (POD) conjugated

anti-mouse IgG in immunoenhancer reagent B (Wako) for 1 h. Then, the specific signals were observed using chemiluminescent substrate (Thermo Fisher Scientific inc., Waltham, MA) and LAS4000 (GE Healthcare), as previously described [28]. The intensities of the bands were quantified with Fujifilm Image Gauge Software.

Rluc assay

HEK293 cells were transiently transfected with each Rluc-fusion-protein expression vector and cultured for 48 h. The harvested cells (1 x 10^5 cells) were lysed with the cell culture lysis reagent (Promega, Madison, WI). To measure Rluc activity, each lysate was transferred to a 96-well white microplate and coelenterazine h [29] was added at a final concentration of 5 μM. Then, luminescence was measured simultaneously using a Wallac ARVO™ SX 1420 luminometer (Perkin-Elmer, Waltman, MA).

Flow cytometry

HEK293/CD4/$Nef_{JR\text{-}CSF}$, HEK293/CD4/$Nef_{NL4\text{-}3}$, HEK293/CD4/$Nef_{JR\text{-}CSF}$ G2A, and HEK293/CD4/$Nef_{NL4\text{-}3}$ G2A cells were washed with PBS and then suspended in a cold washing buffer (PBS containing 2% FCS and 0.02% NaN_3) containing a phycoerythrin (PE)-conjugated anti-CD4 antibody. After 30 min of incubation at 4°C, the cells were washed three times and then analyzed using an EPICS XL flow cytometer (Beckman Coulter).

Quantification of mRNA levels by RT-qPCR analysis

HEK293 cells were transfected with the $Nef_{NL4\text{-}3}$, $Nef_{JR\text{-}CSF}$, AA129-206-EGFP, CP-EGFP, or EGFP expression plasmid. Total RNA was extracted from these HEK293 cells using ISOGEN (Nippon Gene Co., Ltd., Tokyo, Japan) in accordance with to the manufacturer's instruction. First-strand cDNA synthesis was performed using the SuperScript™ III First-Strand Synthesis System for RT-PCR (Invitrogen, Carlsbad, CA) according to the manufacturer's instruction. DyNAmo™ HS SYBR®Green qPCR kit (FINNZYMES, Espoo, Finland) reagents were used as quantitative real-time PCR reagents according to the manufacturer's instruction. Thermocycling was carried out using the DNA Engine OPTICON®2 system (MJ Research, Inc, Waltham, MA). mRNA level was normalized to the transcript of the neomycin resistance gene, which is coded in the expression vector used. The oligonucleotide primers used for the PCR were as follows: a V5 tag sense primer, TCCTCGGTCTCGATTCTACG; a V5 tag antisense primer, TGGATCCTGGTACTCAATGGT; an EGFP sense primer, ACGTAAACGGCCACAAGTTC; an EGFP antisense primer, AAGTCGTGCTGCTTCATGTG; a NeoR sense primer, AGACAATCGGCTGCTCTGAT; and a NeoR antisense primer, AGTGACAACGTCGAGCACAG.

Results and Discussion

Detection of expression diversity of Nef proteins from small subset of HIV-1 and SIV

In the beginning of this study, we constructed expression vectors of Nef from HIV-$1_{NL4\text{-}3}$, HIV-$1_{JR\text{-}CSF}$, HIV-$1_{YU\text{-}2}$, HIV-$1_{89.6}$, and SIV_{mac239} for mammalian cells, which were appended to a V5 epitope tag at the *C*-terminal end for detection. The expression pattern of each Nef was examined at the same time. HEK293 cells transiently expressing each Nef were lysed and subjected to SDS-PAGE, followed by western blot analysis using an anti-V5 antibody, as described in Materials and Methods. As shown in Fig. 1A, the expression of each Nef variant from HIV-$1_{NL4\text{-}3}$, HIV-$1_{JR\text{-}CSF}$, HIV-$1_{YU\text{-}2}$, HIV-$1_{89.6}$, and SIV_{mac239}, were observed, in which the molecular weights of the variants were expectedly detected as 27, 29, 28, 27, and 34 kDa, respectively. Then, in spite of the fact that the same conditions in terms of the type of cell, the amount of DNA for transfection, the expression vector with the CMV promoter, and the V5 epitope for detection were used, the diversity of the expression level among the five Nef's was observed (Figure 1A). We paid attention to the heterogeneity of the expression level. We again examined the expression properties of $Nef_{NL4\text{-}3}$ and $Nef_{JR\text{-}CSF}$, respectively showing the lowest and highest expression levels, using clones of HEK293/CD4 cells stably expressing each Nef. For the expression of these proteins, the pcDNA4/HisMax vector was used, which codes for a strong translational enhancer element [30] upstream of the ATG initiation codon of Nef, and by which an increase in Nef expression level is expected. As shown in Figure 1B, the marked differences between $Nef_{NL4\text{-}3}$ and $Nef_{JR\text{-}CSF}$ were reproducibly observed among the clones tested by western blot analysis; the expression levels of $Nef_{JR\text{-}CSF}$ were more than tenfold those of $Nef_{NL4\text{-}3}$. Relatively low expression levels of $Nef_{NL4\text{-}3}$ were still observed, although the vector with the translational enhancer element was used.

We also examined the expression property by immunostaining HEK293/CD4 cells stably expressing Nef. Nef and the nucleus were respectively stained with an anti-V5 antibody and DAPI, simultaneously. Then, it was verified at a glance that all the cells expressed Nef in both clones (Figure 2). $Nef_{NL4\text{-}3}$ was predominantly detected in some of the focused areas, especially in the perinuclear region (Figure 2, top panels), which is a typical pattern of the subcellular localization of Nef [31, 32]. The regions seemed to include the *trans*-Golgi network, as previously reported [31, 32], although we have not checked for the marker by double staining. On the other hand, $Nef_{JR\text{-}CSF}$ was detected in not only the perinuclear area but also other cytosolic areas with a relatively higher fluorescence (Figure 2, bottom panels). The difference in expression level in the western blot analysis between $Nef_{JR\text{-}CSF}$ and $Nef_{NL4\text{-}3}$ (Figure 1B) was reflected in the result of the immunostaining of